Probing Neutral Triple Gauge Couplings with $Z^*\gamma(\nu\bar{\nu}\gamma)$ Production at Hadron Colliders

John Ellis [a], **Hong-Jian He** [b], **Rui-Qing Xiao** [c]

[a] Department of Physics, King's College London, Strand, London WC2R 2LS, UK;
Theoretical Physics Department, CERN, CH-1211 Geneva 23, Switzerland;
T. D. Lee Institute, Shanghai Jiao Tong University, Shanghai, China

[b] T. D. Lee Institute and School of Physics & Astronomy,
Key Laboratory for Particle Astrophysics and Cosmology,
Shanghai Key Laboratory for Particle Physics and Cosmology,
Shanghai Jiao Tong University, Shanghai, China;
Physics Department & Institute of Modern Physics, Tsinghua University, Beijing, China;
Center for High Energy Physics, Peking University, Beijing, China

[c] Department of Physics, King's College London, Strand, London WC2R 2LS, UK;
T. D. Lee Institute and School of Physics & Astronomy,
Shanghai Jiao Tong University, Shanghai, China

(john.ellis@cern.ch, hjhe@sjtu.edu.cn, xiaoruiqing@sjtu.edu.cn)

arXiv:2308.16887v4 [hep-ph] 31 Dec 2023

Abstract

We study probes of neutral triple gauge couplings (nTGCs) via $Z^*\gamma$ production followed by off-shell decays $Z^*\to\nu\bar{\nu}$ at the LHC and future *pp* colliders, including both CP-conserving (CPC) and CP-violating (CPV) couplings. We present the dimension-8 SMEFT operators contributing to nTGCs and derive the correct form factor formulation for the off-shell vertices $Z^*\gamma V^*$ $(V=Z,\gamma)$ by matching them with the dimension-8 SMEFT operators. Our analysis includes new contributions enhanced by the large off-shell momentum of Z^*, beyond those of the conventional $Z\gamma V^*$ vertices with on-shell $Z\gamma$. We analyze the sensitivity reaches for probing the CPC/CPV nTGC form factors and the new physics scales of the dimension-8 nTGC operators at the LHC and future 100 TeV *pp* colliders. We compare our new predictions with the existing LHC measurements of CPC nTGCs in the $\nu\bar{\nu}\gamma$ channel and demonstrate the importance of our new method.

KCL-PH-TH/2023-39, CERN-TH-2023-129

Phys. Rev. D (Letter) 108 (2023) L111704, no.11 [arXiv:2308.16887]

1. Introduction

Neutral triple gauge couplings (nTGCs) are attracting increased theoretical and experimental interest [1][2][3][4][5][6]. This is largely driven by the fact [7][8] that the nTGCs do not appear in the Standard Model (SM) Lagrangian, nor do they show up in the dimension-6 Lagrangian of the SM Effective Field Theory (SMEFT) [10], suggesting that they could open up a unique new window to physics beyond the SM that may first appear at the dimension-8 level. The SMEFT provides a powerful universal framework to formulate model-independently such new physics beyond the SM, by parametrizing the low-energy effects of possible high-mass new physics in terms of operators composed of the SM fields that incorporate the full SU(3)⊗SU(2)⊗U(1) gauge symmetry of the SM.

There have been extensive studies of the dimension-6 operators [10][11][12] in the SMEFT, including the experimental constraints on their coefficients and hence on the associated new physics cutoff scale Λ. But these studies do not involve nTGCs because they first appear as a set of dimension-8 operators of the SMEFT. In general, dimension-8 operators make interference contributions to amplitudes at $O(1/\Lambda^4)$, and thus can contribute to cross sections at the same order. But dimension-6 SMEFT operators contributing to amplitudes at $O(1/\Lambda^2)$ also contribute to cross sections at $O(1/\Lambda^4)$ in general, complicating efforts to isolate any dimension-8 contributions. The absence of dimension-6 contributions to nTGCs avoids this complication, making them an ideal place to probe the new physics at dimension-8 level.

Previous phenomenological studies of nTGCs in the SMEFT formalism have mainly focused on CP-conserving (CPC) operators that contribute to scattering amplitudes involving the neutral triple gauge vertex (nTGV) $Z\gamma V^*$ $(V = Z, \gamma)$ through the reaction $f\bar{f} \to Z\gamma$. In the case of e^+e^- colliders, on-shell $Z\gamma$ production with $Z \to \ell^-\ell^+, \nu\bar{\nu}, q\bar{q}$ final states have been considered, but at pp colliders off-shell invisible decays $Z^* \to \nu\bar{\nu}$ cannot be separated from on-shell Z decays because of the insufficient kinematic information of Z boson. Hence, for the $\nu\bar{\nu}\gamma$ channel it is important to include the off-shell production of $Z^* \to \nu\bar{\nu}$ at pp colliders.

In this work, we study the nTGVs with two off-shell bosons, $Z^*\gamma V^*$ $(V = Z, \gamma)$, which include contributions from additional dimension-8 operators that were not considered in the previous nTGC studies. We include a new analysis of CP-violating (CPV) nTGCs. As the basis for this work, we first formulate the correct CPC and CPV form factors of the doubly off-shell nTGVs $Z^*\gamma V^*$ that are compatible with the full electroweak SU(2)⊗U(1) gauge symmetry of the SM [13]. By matching the CPC and CPV dimension-8 nTGC operators with the corresponding nTGC form factors, we derive the correct formulations of the CPC and CPV $Z^*\gamma V^*$ form factors. We then use these formulations to study the sensitivity reaches of the LHC and the projected 100 TeV pp colliders for probing the CPC and CPV nTGCs through the reaction $pp(q\bar{q}) \to Z^*\gamma \to \nu\bar{\nu}\gamma$. We further compare our new predictions with the existing LHC measurements [5] of CPC nTGCs in the $\nu\bar{\nu}\gamma$ channel, and demonstrate the importance of using our new nTGC form factor formulation for the correct LHC experimental analysis.

2. Formulating $Z^*\gamma V^*$ Form Factors from Matching the SMEFT

In previous works [1][2][3], we studied the dimension-8 SMEFT operators that generate nTGCs and their contributions to $Z\gamma$ production at the LHC and future colliders. In particular, we studied systematically $Z\gamma V^*$ vertices including their matching with the corresponding SMEFT operators and the correct formulation of nTGC form factors that respect the full electroweak

SU(2)⊗U(1) gauge symmetry of the SM. However, unlike the case of e^+e^- collisions where the on-shell constraint can be imposed on the invisible decays of $Z\to\nu\bar{\nu}$, this is not possible in pp collisions, for which only the missing transverse momentum can be measured. Moreover, since Z boson is an unstable particle, the invariant-masses of $\ell^+\ell^-$ and $q\bar{q}$ final states from Z decays are not exactly on-shell, in general. For these reasons, it is important to study the nTGVs with the final-state Z^* off-shell, as well as the initial-state V^*.

The general dimension-8 SMEFT Lagrangian takes the following form:

$$\Delta\mathcal{L}(\text{dim-8}) = \sum_j \frac{\tilde{c}_j}{\tilde{\Lambda}^4}\mathcal{O}_j = \sum_j \frac{\text{sign}(\tilde{c}_j)}{\Lambda_j^4}\mathcal{O}_j = \sum_j \frac{1}{[\Lambda_j^4]}\mathcal{O}_j\,, \tag{2.1}$$

where the dimensionless coefficients $\tilde{c}_j$ may take either sign, $\text{sign}(\tilde{c}_j)=\pm$. For each dimension-8 operator $\mathcal{O}_j$, we define in Eq.(2.1) the corresponding effective cutoff scale for new physics, $\Lambda_j \equiv \tilde{\Lambda}/|\tilde{c}_j|^{1/4}$, and introduce the notation $[\Lambda_j^4] \equiv \text{sign}(\tilde{c}_j)\Lambda_j^4$.

The following CPC and CPV nTGC operators include Higgs doublets:

$$\begin{aligned}
&\text{CPC:} \quad \mathcal{O}_{\widetilde{B}W} = \mathrm{i}\, H^\dagger \widetilde{B}_{\mu\nu} W^{\mu\rho} \{D_\rho, D^\nu\} H + \text{h.c.}, && \text{(2.2a)}\\
&\text{CPC:} \quad \mathcal{O}_{\widetilde{BW}} = \mathrm{i}\, H^\dagger \big(D_\sigma \widetilde{W}^a_{\mu\nu} W^{a\mu\sigma} + D_\sigma \widetilde{B}_{\mu\nu} B^{\mu\sigma}\big) D^\nu H + \text{h.c.}, && \text{(2.2b)}\\
&\text{CPV:} \quad \widetilde{\mathcal{O}}_{BW} = \mathrm{i}\, H^\dagger B_{\mu\nu} W^{\mu\rho} \{D_\rho, D^\nu\} H + \text{h.c.}, && \text{(2.2c)}\\
&\text{CPV:} \quad \widetilde{\mathcal{O}}_{WW} = \mathrm{i}\, H^\dagger W_{\mu\nu} W^{\mu\rho} \{D_\rho, D^\nu\} H + \text{h.c.}, && \text{(2.2d)}\\
&\text{CPV:} \quad \widetilde{\mathcal{O}}_{BB} = \mathrm{i}\, H^\dagger B_{\mu\nu} B^{\mu\rho} \{D_\rho, D^\nu\} H + \text{h.c.}, && \text{(2.2e)}
\end{aligned}$$

where H denotes the Higgs doublet of the SM, and the covariant derivative term $D_\sigma \widetilde{B}_{\mu\nu} = \partial_\sigma \widetilde{B}_{\mu\nu}$ holds for the Abelian field strength. The operators (2.2a) and (2.2c)-(2.2e) were given in [8], to which we have further added an independent CPC operator (2.2b).

For the dimension-8 CPC and CPV nTGC operators containing pure gauge fields only, we have the following:

$$\begin{aligned}
&\text{CPC:} \quad g\mathcal{O}_{G+} = \widetilde{B}_{\mu\nu} W^{a\mu\rho}(D_\rho D_\lambda W^{a\nu\lambda} + D^\nu D^\lambda W^a_{\lambda\rho}), && \text{(2.3a)}\\
&\text{CPC:} \quad g\mathcal{O}_{G-} = \widetilde{B}_{\mu\nu} W^{a\mu\rho}(D_\rho D_\lambda W^{a\nu\lambda} - D^\nu D^\lambda W^a_{\lambda\rho}), && \text{(2.3b)}\\
&\text{CPV:} \quad g\widetilde{\mathcal{O}}_{G+} = B_{\mu\nu} W^{a\mu\rho}(D_\rho D_\lambda W^{a\nu\lambda} + D^\nu D^\lambda W^a_{\lambda\rho}), && \text{(2.3c)}\\
&\text{CPV:} \quad g\widetilde{\mathcal{O}}_{G-} = B_{\mu\nu} W^{a\mu\rho}(D_\rho D_\lambda W^{a\nu\lambda} - D^\nu D^\lambda W^a_{\lambda\rho}), && \text{(2.3d)}
\end{aligned}$$

where the operators $(\mathcal{O}_{G+}, \mathcal{O}_{G-})$ are CPC [2], and the two new CPV operators $(\widetilde{\mathcal{O}}_{G+}, \widetilde{\mathcal{O}}_{G-})$ are constructed. We note that the operators (2.2)-(2.3) belong to the two classes, $F^2\phi^2D^2$ and F^3D^2. From the classification of [9] the relevant dimension-8 operators contains $F^2H^2D^2$, $F^2\psi^2D$, and F^4, where $F^2\psi^2D$ and F^4 do not explicitly contain any nTGC vertices and thus are not included here. Using integration by parts and equations of motion (EOM), we find that F^3D^2 type can be converted into three types of operators (F^4, $F^2\psi^2D$, $F^2H^2D^2$), where $F^2H^2D^2$ corresponds to our Eq.(2.2). Moreover, the $F^2H^2D^2$ type operators contribute to the form factors (h_3^V, h_1^V) only, but not to (h_4^V, h_2^V), as shown by Eqs.(2.6)(2.8) below. Hence, the operator types $F^2\phi^2D^2$ and F^3D^2 provide the optimal basis for the current nTGC study. These are further explained in Sec. S1 of the Supplemental Material [21].

The conventional formalism for nTGC form factors was proposed over 20 years ago [7] and respects only the residual gauge symmetry $U(1)_{\text{em}}$. However, as we stressed in Ref. [1], it does not respect the full electroweak SU(2)⊗U(1) gauge symmetry of the SM, and leads to large unphysical high-energy behaviors of certain scattering amplitudes [1]. We thus proposed [1] a new formulation of the CPC form factors of the nTGVs $Z\gamma V^*$ that is compatible with the full SM gauge group with spontaneous electroweak symmetry breaking. We will construct an extended formulation to include the CPV nTGVs for the present study.

The doubly off-shell nTGC form factors for $Z^*\gamma V^*$ vertices are more complicated than the $Z\gamma V^*$ form factors. Matching with the dimension-8 nTGC operators of the SMEFT, we can parametrize the $Z^*\gamma V^*$ vertices in terms of the following form factors:

$$V_{Z^*\gamma V^*}^{\alpha\beta\mu} = \Gamma_{Z^*\gamma V^*}^{\alpha\beta\mu} + \frac{e}{M_Z^2} q_1^\alpha X_{1V}^{\beta\mu} + \frac{e}{M_Z^2} q_3^\mu X_{3V}^{\alpha\beta}\,, \tag{2.4}$$

where expressions for $X_{1V}^{\beta\mu}$ and $X_{3V}^{\alpha\beta}$ are given in Appendix S1 and we find that they make vanishing contributions to the reaction $f\bar{f} \to Z^{(*)}\gamma$ with $Z^{(*)} \to f'\bar{f}'$. Hence, the present analysis only involves the vertices $\Gamma_{Z^*\gamma V^*}^{\alpha\beta\mu}$.

We present first the CPC parts of the $\Gamma_{Z^*\gamma V^*}^{\alpha\beta\mu}$ vertices:

$$\Gamma_{Z^*\gamma\gamma^*}^{\alpha\beta\mu}(q_1,q_2,q_3) = \frac{e}{M_Z^2}\left(h_{31}^{\gamma} + \frac{\hat{h}_3^{\gamma} q_1^2}{M_Z^2}\right) q_3^2 q_{2\nu}\epsilon^{\alpha\beta\mu\nu} + \frac{e s_W \hat{h}_4 q_3^2}{2c_W M_Z^4}\left(2q_2^\alpha q_{3\nu} q_{2\sigma}\epsilon^{\beta\mu\nu\sigma} + q_3^2 q_{2\nu}\epsilon^{\alpha\beta\mu\nu}\right), \tag{2.5a}$$

$$\Gamma_{Z^*\gamma Z^*}^{\alpha\beta\mu}(q_1,q_2,q_3) = \frac{e(q_3^2 - q_1^2)}{M_Z^2}\left[\hat{h}_3^Z q_{2\nu}\epsilon^{\alpha\beta\mu\nu} + \frac{\hat{h}_4}{2M_Z^2}\left(2q_2^\alpha q_{3\nu} q_{2\sigma}\epsilon^{\beta\mu\nu\sigma} + q_3^2 q_{2\nu}\epsilon^{\alpha\beta\mu\nu}\right)\right]. \tag{2.5b}$$

In the above, we use the hat symbol to distinguish off-shell form factors $(\hat{h}_3^Z, \hat{h}_3^\gamma, \hat{h}_4)$ from their on-shell counterparts (h_3^γ, h_3^Z, h_4) as studied in [1]. The CPC form-factor parameters $(h_{31}^\gamma, \hat{h}_3^\gamma, \hat{h}_3^Z, \hat{h}_4)$ can be mapped precisely to the cutoff scales $(\Lambda_{\widetilde{BW}}, \Lambda_{\tilde{B}W}, \Lambda_{G-}, \Lambda_{G+})$ of the dimension-8 operators $(\mathcal{O}_{\widetilde{BW}}, \mathcal{O}_{\tilde{B}W}, \mathcal{O}_{G+}, \mathcal{O}_{G-})$, as follows:

$$\hat{h}_4 = \frac{\hat{r}_4}{[\Lambda_{G+}^4]}, \quad \hat{h}_3^Z = \frac{\hat{r}_3^Z}{[\Lambda_{\tilde{B}W}^4]}, \quad \hat{h}_3^\gamma = \frac{\hat{r}_3^\gamma}{[\Lambda_{G-}^4]}, \quad h_{31}^\gamma = \frac{r_{31}^\gamma}{[\Lambda_{\widetilde{BW}}^4]}, \tag{2.6a}$$

$$\hat{r}_4 = -\frac{v^2 M_Z^2}{s_W c_W}, \quad \hat{r}_3^Z = \frac{v^2 M_Z^2}{2 s_W c_W}, \quad \hat{r}_3^\gamma = -\frac{v^2 M_Z^2}{2c_W^2}, \quad r_{31}^\gamma = -\frac{v^2 M_Z^2}{s_W c_W}, \tag{2.6b}$$

where $[\Lambda_j^4] \equiv \text{sign}(\tilde{c}_j)\Lambda_j^4$. The above relations hold for any momentum q_1 of Z^*, and for $q_1^2 = M_Z^2$ the off-shell form factors $(\hat{h}_3^Z, \hat{h}_3^\gamma, \hat{h}_4)$ reduce to the on-shell cases, $\hat{h}_4 = h_4$, $\hat{h}_3^Z = h_3^Z$, and $\hat{h}_3^\gamma + h_{31}^\gamma = h_3^\gamma$, where h_{31}^γ is part of the on-shell form factor, $h_{31}^\gamma = h_3^\gamma - \hat{h}_3^\gamma$, for $q_1^2 = M_Z^2$.

We note that the formulations of the off-shell nTGC form factors $Z^*\gamma V^*$ in Eq.(2.5) (the CPC case) and in Eq.(2.7) (the CPV case) were not given explicitly in the previous literature, including Refs. [7]-[8]. As we discuss in Section 3, CMS [4] and ATLAS [5] measured the CPC nTGC form factors h_3^γ and h_4^V via the reaction $pp(q\bar{q}) \to Z^*\gamma \to \nu\bar{\nu}\gamma$, but used the conventional CPC nTGC form factor formulation of $Z\gamma V^*$ in which both the final-state bosons $Z\gamma$ are assumed to be on-shell [7]. This means that their measurement of h_3^γ is simply equivalent to measuring the form factor h_{31}^γ in Eq.(2.5a) above [14]. Hence the CMS and ATLAS analyses [4][5] missed the new form factor $\hat{h}_3^\gamma$ in Eq.(2.5a), whose contribution dominates over that of h_{31}^γ in the $\nu\bar{\nu}\gamma$ channel for both the LHC and 100 TeV pp colliders, as we will demonstrate in Section 3.

Next, using the Lagrangian (S5) for nTGVs, we construct the following off-shell CPV nTGVs $\Gamma_{Z^*\gamma V^*}^{\alpha\beta\mu}$:

$$\Gamma^{\alpha\beta\mu}_{Z^*\gamma\gamma^*}(q_1,q_2,q_3) = \frac{e}{M_Z^2}\left(h_{11}^{\gamma}+\frac{\hat{h}_1^{\gamma}q_1^2}{M_Z^2}\right)q_3^2\left(q_2^{\alpha}g^{\mu\beta}-q_2^{\mu}g^{\alpha\beta}\right)+\frac{e\,s_W\hat{h}_2q_3^2}{2c_WM_Z^4}\left(q_1^2q_2^{\alpha}g^{\mu\beta}-q_3^2q_2^{\mu}g^{\alpha\beta}\right), \tag{2.7a}$$

$$\Gamma^{\alpha\beta\mu}_{Z^*\gamma Z^*}(q_1,q_2,q_3) = \frac{e\,(q_3^2-q_1^2)}{M_Z^2}\left[\hat{h}_1^Z\left(q_2^{\alpha}g^{\mu\beta}-q_2^{\mu}g^{\alpha\beta}\right)+\frac{\hat{h}_2}{2M_Z^2}\left(q_1^2q_2^{\alpha}g^{\mu\beta}-q_3^2q_2^{\mu}g^{\alpha\beta}\right)\right], \tag{2.7b}$$

which have important differences from the conventional CPV nTGC form factors [7] as we explain in Appendix S1. We note that when the final-state Z boson is on-shell ($q_1^2=M_Z^2$), the above off-shell form factors should reduce to the on-shell ones, $h_{11}^{\gamma}+\hat{h}_1^{\gamma}=h_1^{\gamma}$, $\hat{h}_1^Z=h_1^Z$, and $\hat{h}_2=h_2$. In the on-shell limit, the longitudinally polarized on-shell external state $Z_L(q_1)$ should satisfy the equivalence theorem (ET) [15], which puts nontrivial constraints on the structure of form factors, as shown in Appendix S1.

Then, we can match these CPV nTGC form factors to the dimension-8 gauge-invariant CPV operators (2.2)-(2.3) in the broken phase and derive the following correspondence relations:

$$\hat{h}_1^Z = v^2M_Z^2\left(-\frac{1}{4[\Lambda_{WW}^4]}+\frac{c_W^2-s_W^2}{4c_Ws_W[\Lambda_{WB}^4]}+\frac{1}{[\Lambda_{BB}^4]}\right), \tag{2.8a}$$

$$h_{11}^{\gamma} = v^2M_Z^2\left(-\frac{s_W}{4c_W[\Lambda_{WW}^4]}+\frac{1}{2[\Lambda_{WB}^4]}-\frac{c_W}{s_W[\Lambda_{BB}^4]}\right), \tag{2.8b}$$

$$\hat{h}_1^{\gamma} = \frac{v^2M_Z^2}{4c_W^2[\Lambda_{\widetilde{G}-}^4]}, \tag{2.8c}$$

$$\hat{h}_2 = -\frac{v^2M_Z^2}{2s_Wc_W[\Lambda_{\widetilde{G}+}^4]}. \tag{2.8d}$$

We find that the Higgs-field-dependent CPV operators (2.2c)-(2.2e) can generate the form factors (h_{11}^{γ}, h_1^Z), where h_{11}^{γ} is part of the on-shell form factor $h_1^{\gamma}=h_{11}^{\gamma}+\hat{h}_1^{\gamma}$.

In summary, there are eight independent CPC and CPV form factors for the nTGC vertices $Z^*\gamma V^*$. These can be mapped to the four CPC operators (2.2a)-(2.2b),(2.3a)-(2.3b) and the five CPV operators (2.2c)-(2.2e),(2.3c)-(2.3d). In the case of $Z\gamma V^*$ vertices with on-shell Z and γ, there are only six independent parameters because $h_{31}^{\gamma}+\hat{h}_3^{\gamma}=h_3^{\gamma}$ and $h_{11}^{\gamma}+\hat{h}_1^{\gamma}=h_1^{\gamma}$. Matching the nTGC form factors with the corresponding dimension-8 operators of the SMEFT, we observe that the ($h_{11}^{\gamma}, h_{31}^{\gamma}$) and ($\hat{h}_1^Z, \hat{h}_3^Z$) form factors arise as a consequence of spontaneous electroweak symmetry breaking, and would vanish if $\langle H\rangle=0$. We also note that $\hat{h}_{1,3}^{\gamma}$ and $\hat{h}_{2,4}$ arise from the electroweak rotation of the BW^3W^3 vertex, so the $\hat{h}_1^{\gamma}$ term in Eq.(2.7a) and $\hat{h}_3^{\gamma}$ term in Eq.(2.5a) would vanish if $s_W=0$.

In passing, we have also derived the perturbative unitarity bounds on the cutoff scales Λ_j and the form factors h_j^V in Section S3 of the Supplemental Material. We verify that these bounds are much weaker than our current collider limits (presented in Section 3) and thus do not affect our collider analyses.

3. Probing nTGCs with $Z^*\gamma(\nu\bar{\nu}\gamma)$ Production at Hadron Colliders

The invariant mass of $Z^{(*)}\!\to\nu\bar{\nu}$ decays cannot be measured in the reaction $pp(q\bar{q})\to\nu\bar{\nu}\gamma$ at hadron colliders, so it becomes impossible to determine whether the invisible Z-decay is on-

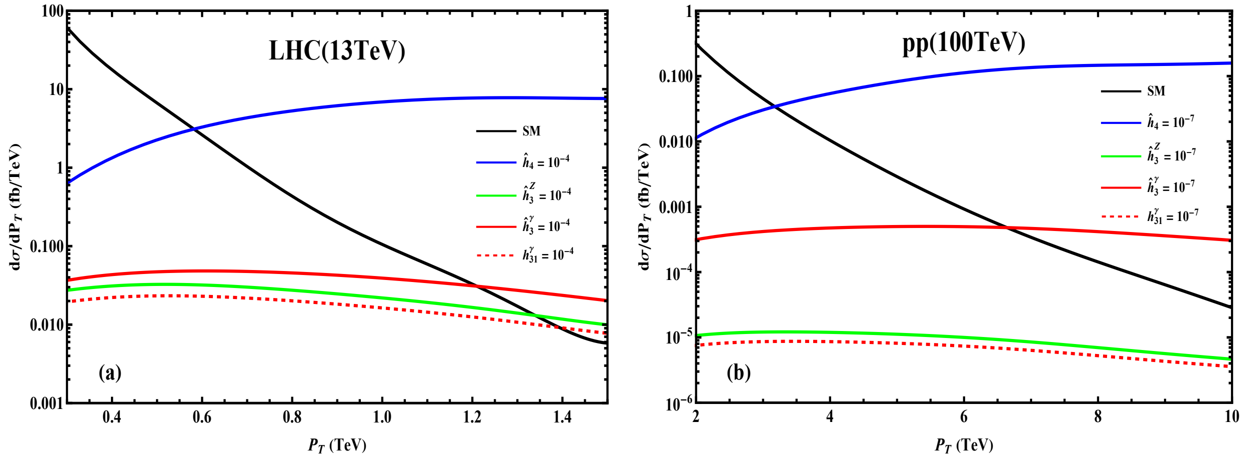

Figure 1: *Differential cross sections for $\nu\bar{\nu}\gamma$ production as functions of the photon transverse momentum P_T^γ, shown in plot (a) for the* LHC (13 TeV) *and in plot (b) for the projected* 100 TeV *pp collider. In each plot, the SM cross section is given by a black curve, and the contributions of the different nTGC form factors (taking a reference value 10^{-4}) are shown by the colored curves.*

shell or not. Hence analyzing the $\nu\bar{\nu}\gamma$ production with off-shell Z^* decays is important for hadron colliders.

The cross section for $q\bar{q} \to Z^{(*)}\gamma$ at a pp collider can be expressed as

$$\sigma \;=\; \sum_{q,\bar{q}} \int \mathrm{d}x_1 \mathrm{d}x_2 \big[\mathcal{F}_{q/p}(x_1,\mu)\mathcal{F}_{\bar{q}/p}(x_2,\mu)\,\sigma_{q\bar{q}}(\hat{s}) + (q \leftrightarrow \bar{q})\big]\,, \tag{3.1}$$

where the functions $\mathcal{F}_{q/p}$ and $\mathcal{F}_{\bar{q}/p}$ are the parton distribution functions (PDFs) of the quark and antiquark in the proton beams, and $\hat{s} = x_1 x_2 s$. The PDFs depend on the factorization scale μ, which we set to $\mu = \sqrt{\hat{s}}/2$ in our leading-order analysis. We use the PDFs of the quarks $q = u, d, s, c, b$ and their antiquarks determined by the CTEQ collaboration [16]. In principle, $\hat{s}$ can be determined by measuring the invariant-mass of observable final-state particles. ATLAS measurements of $M_{\ell\ell\gamma}$ during the LHC Run-2 reached around 3 TeV. Accordingly, in our analysis of $Z^*\gamma(\nu\bar{\nu}\gamma)$ production we consider the relevant range $\hat{s} < 3$ TeV for the LHC and $\hat{s} < 23$ TeV for a 100 TeV pp collider.

We compute the partonic cross-section in three parts,

$$\sigma(q\bar{q} \to Z^*\gamma) \;=\; \sigma_0 + \sigma_1 + \sigma_2\,, \tag{3.2}$$

where σ_0 is the SM contribution, σ_1 is the contribution of the nTGCs interfering with the SM amplitude, and σ_2 denotes the squared nTGC contribution. We present explicit formulae for $(\sigma_0, \sigma_1, \sigma_2)$ in Appendix S2. The CPC and CPV amplitudes do not interfere for $q\bar{q} \to Z^{(*)}\gamma$, hence the contributions of the CPV nTGCs to σ_1 vanish. Moreover, we find that $\sigma_1 \ll \sigma_2$ holds for the CPC nTGCs at the LHC and future pp colliders, making σ_1 negligible in this analysis [17]. We further observe that each CPV nTGC gives the same contribution to σ_2 as that of the corresponding CPC nTGC.

The final state γ is the only visible particle when $Z^{(*)}$ has invisible decays, and the longitudinal momentum of the $\nu\bar{\nu}$ pair cannot be measured at hadron colliders. Hence, the photon's transverse momentum P_T^γ is the main variable that can be used to distinguish the new physics signals from the SM backgrounds. We present in Fig. 1 distributions of the $Z^*\gamma$ cross section

$\sqrt{s}$	13 TeV				100 TeV		
$\mathcal{L}(\text{ab}^{-1})$	0.14	0.3	3		3	10	30
$\lvert\hat{h}_{4,2}\rvert\times 10^6$	11	8.5	4.2	$\lvert\hat{h}_{4,2}\rvert\times 10^9$	4.5	2.9	2.0
$\lvert\hat{h}^Z_{3,1}\rvert\times 10^4$	2.2	1.7	0.90	$\lvert\hat{h}^Z_{3,1}\rvert\times 10^7$	7.0	4.8	3.4
$\lvert\hat{h}^\gamma_{3,1}\rvert\times 10^4$	1.6	1.3	0.67	$\lvert\hat{h}^\gamma_{3,1}\rvert\times 10^7$	0.94	0.62	0.44
$\lvert h^\gamma_{31,11}\rvert\times 10^4$	2.5	2.0	1.0	$\lvert h^\gamma_{31,11}\rvert\times 10^7$	8.3	5.7	4.0

Table 1: *Sensitivity reaches on probing the CPC and CPV nTGC form factors at the* 2σ *level, as obtained by analyzing the reaction* $pp(q\bar{q})\to Z^*\gamma\to\nu\bar{\nu}\gamma$ *at the* LHC (13 TeV) *and the* 100 TeV *pp collider, for the indicated integrated luminosities. In the last two rows, the* $\hat{h}^\gamma_{3,1}$ *sensitivities (red color) include the* Z^**-momentum-square* (q_1^2) *enhanced off-shell effects, whereas the* $h^\gamma_{31,11}$ *sensitivities (blue color) do not.*

for the LHC (13 TeV) in plot (a) and for the projected 100 TeV *pp* collider in plot (b). In each plot, the SM cross section is given by the black curve, and the contributions of the nTGC form factors ($\hat{h}_4, \hat{h}_3^Z, \hat{h}_3^\gamma, h_{31}^\gamma$) (taking a reference value 10^{-4}) are shown by the blue, green, red and red-dashed curves. We observe from Eq.(2.5a) that the $\hat{h}_3^\gamma$ contribution is strongly enhanced by the off-shell Z^* momentum factor q_1^2/M_Z^2, whereas the $\hat{h}_{31}^\gamma$ contribution is not. Unlike $\hat{h}_3^\gamma$, this does not happen to $\hat{h}_3^Z$ because Eq.(2.5b) shows that the numerator factor $q_3^2-q_1^2$ exhibits a strong cancellation between $q_3^2\,(=\hat{s})$ and q_1^2 when q_1^2 goes far off-shell, which is particularly relevant for the high-energy 100 TeV *pp* collider. We find that the $\hat{h}_3^\gamma$ contribution (red solid curve) is larger than that of $\hat{h}_{31}^\gamma$ (red dashed curve) by about a factor of $(2-3)$ for the LHC, as seen in Fig. 1(a), and by a large factor of $(43-77)$ in the case of the 100 TeV *pp* collider, as seen in Fig. 1(b). We note that the $\hat{h}_4$ contribution is much larger than that of $\hat{h}_3^Z$, $\hat{h}_3^\gamma$, and h_{31}^γ, because the $\hat{h}_4$ terms are enhanced by an extra large momentum factor of q_2q_3 or q_3^2 , as shown in Eq.(2.5).

In order to optimize the detection sensitivity, we divide events into bins of the $P_T(\gamma)$ distribution, whose widths we take as $\Delta P_T = 100\,\text{GeV}$ for the LHC and $\Delta P_T = 500\,\text{GeV}$ for the 100 TeV *pp* collider. Then, we compute the significance $\mathcal{Z}_{\text{bin}}$ for each bin, and construct the following total significance measure:

$$\mathcal{Z}_{\text{total}} \,=\, \sqrt{\sum \mathcal{Z}_{\text{bin}}^2}\,. \tag{3.3}$$

Since the SM contribution σ_0 becomes small when the photon P_T is high, we determine the statistical significance by using the following formula for the background-with-signal hypothesis [20]:

$$\mathcal{Z} \,=\, \sqrt{2\left(B\ln\frac{B}{B+S}+S\right)} \,=\, \sqrt{2\left(\sigma_0\ln\frac{\sigma_0}{\sigma_0+\Delta\sigma}+\Delta\sigma\right)}\times\sqrt{\mathcal{L}\times\epsilon}\,, \tag{3.4}$$

where $\mathcal{L}$ is the integrated luminosity and ϵ denotes the detection efficiency. For our analysis we choose an ideal detection efficiency $\epsilon = 100\%$ unless specified otherwise.

We present sensitivities for probing the CPC and CPV nTGC form factors and the corresponding new physics scales of the dimension-8 nTGC operators in Tables 1 and 2, respectively. For the LHC, we find that the sensitivities to $\hat{h}_2$ and $\hat{h}_4$ can reach the level of $O(10^{-5}\text{–}10^{-6})$, whereas the sensitivities to $\hat{h}_{3,1}^Z$, $\hat{h}_{3,1}^\gamma$ and $h_{31,11}^\gamma$ are of $O(10^{-4})$. The sensitivities for probing the

$\sqrt{s}$	13 TeV			100 TeV		
$\mathcal{L}\,(\mathrm{ab}^{-1})$	0.14	0.3	3	3	10	30
Λ_{G+}(CPC)	3.2	3.5	4.1	23	25	28
Λ_{G-}(CPC)	1.2	1.3	1.5	7.7	8.5	9.3
$\Lambda_{\widetilde{B}W}$(CPC)	1.3	1.4	1.6	5.4	5.9	6.4
$\Lambda_{\widetilde{BW}}$(CPC)	1.5	1.6	1.8	6.2	6.8	7.4
$\Lambda_{\widetilde{G}+}$(CPV)	2.7	2.9	3.5	19	21	23
$\Lambda_{\widetilde{G}-}$(CPV)	1.0	1.1	1.3	6.5	7.2	7.8
Λ_{WW}(CPV)	0.93	0.98	1.2	3.9	4.3	4.6
Λ_{WB}(CPV)	1.1	1.2	1.4	4.6	5.1	5.5
Λ_{BB}(CPV)	1.3	1.4	1.7	5.6	6.2	6.8

Table 2: *Sensitivity reaches on probing the new physics scales Λ_j (TeV) of the dimension-8 nTGC operators at 2σ level, as derived by analyzing the reaction $pp(q\bar{q})\!\to\! Z^*\gamma\!\to\!\nu\bar{\nu}\gamma$ at the* LHC (13 TeV) *and at a* 100 TeV *pp collider, with the integrated luminosities $\mathcal{L}$ as shown in this table.*

nTGC form factors at the projected 100 TeV pp collider are generally much higher than those at the LHC, by a factor of $O(10^2\!-\!10^3)$. At the LHC the sensitivities to $\hat{h}_{3,1}^{\gamma}$ are stronger than those to $h_{31,11}^{\gamma}$ and $\hat{h}_{3,1}^{Z}$ by about (50–60)%, whereas at the 100 TeV pp collider the sensitivities to $\hat{h}_{3,1}^{\gamma}$ are much higher than those to $h_{31,11}^{\gamma}$ and $\hat{h}_{3,1}^{Z}$, by factors of $O(10)$.

We recall that both CMS (using 19.6/fb of Run-1 data) [4] and ATLAS (using 36.9/fb of Run-2 data) [5] measured the CPC nTGC form factors $(h_3^V,\, h_4^V)$ via the reaction $pp(q\bar{q})\to Z^*\gamma\!\to\!\nu\bar{\nu}\gamma$; but they used the conventional CPC nTGC form factor formulation of the $Z\gamma V^*$ vertex with both $Z\gamma$ being on-shell [7]. This differs from our off-shell formulation of the $Z^*\gamma V^*$ vertex in Eq.(2.5), which gives the correct nTGC form factor formulation for analyzing the reaction $pp(q\bar{q})\!\to\! Z^*\gamma\!\to\!\nu\bar{\nu}\gamma$ at hadron colliders. For instance, using 36.1/fb of Run-2 data at the LHC (13 TeV), ATLAS obtained the following bounds at 95% C.L. [5]:

$$\begin{aligned} h_3^{\gamma} &\in (-3.7,\, 3.7)\times 10^{-4}\,, \qquad & h_3^{Z} &\in (-3.2,\, 3.3)\times 10^{-4}\,,\\ h_4^{\gamma} &\in (-4.4,\, 4.3)\times 10^{-7}\,, \qquad & h_4^{Z} &\in (-4.5,\, 4.4)\times 10^{-7}\,. \end{aligned} \tag{3.5}$$

For a quantitative comparison, we impose the same cut $P_T^{\gamma}\!>\!600\,\mathrm{GeV}$ as that of the ATLAS analysis [5] and choose a detection efficiency $\epsilon\!=\!70\%$ [5][19]. We then derive the following LHC bounds on the CPC nTGCs at 95% C.L.:

$$|h_{31}^{\gamma}| < 3.5\times 10^{-4}\,, \quad |\hat{h}_3^{\gamma}| < 2.3\times 10^{-4}\,, \quad |\hat{h}_3^{Z}| < 3.1\times 10^{-4}\,, \quad |\hat{h}_4| < 1.4\times 10^{-5}\,. \tag{3.6}$$

Comparing our results (3.6) with the ATLAS result (3.5), we find that our bounds on h_{31}^{γ} and $\hat{h}_3^{Z}$ agree well with the ATLAS bounds on h_3^{γ} and h_3^{Z} (to within a few percent), whereas our bound on $\hat{h}_3^{\gamma}$ is significantly stronger than the ATLAS bound on h_3^{γ} by about 60%. This is because in our off-shell formulation of Eq.(2.5) the form factor $\hat{h}_3^{\gamma}$ is enhanced by the Z^* off-shell factor q_1^2/M_Z^2, but h_{31}^{γ} and $\hat{h}_3^{Z}$ are not and thus their bounds are quite similar to the case of assuming on-shell invisible Z decays. On the other hand, our $\hat{h}_4$ bound in Eq.(3.6) is much weaker than the ATLAS bounds on (h_4^{γ}, h_4^{Z}), by a large factor of $\sim\!32$, because the conventional nTGC form factor formulae are incompatible with the gauge-invariant SMEFT formulation of dimension-8 (including spontaneous electroweak gauge symmetry breaking), as we explain in Appendix S1 and Table S3. We emphasize that the existing ATLAS result [5] used the conventional on-shell nTGC formula of the vertex $Z\gamma V^*$ [7] for analyzing the $\nu\bar{\nu}\gamma$ channel, which caused a significant underestimate of the sensitivity to $\hat{h}_3^\gamma$ by about 60%. This underlines the importance for the on-going LHC experimental analyses to use *the correct theoretical formalism* to analyze the $\nu\bar{\nu}\gamma$ channel for probing the nTGCs, as proposed in this work.

In Table 2 we demonstrate that the sensitivities to new physics scales in the coefficients of $\mathcal{O}_{G+}$ and $\widetilde{\mathcal{O}}_{G+}$ can reach $(2.7-4.1)$ TeV at the LHC, and $(19-28)$ TeV at the 100 TeV pp collider. The sensitivities to probing new physics scales of other nTGC operators are around $(1-1.8)$ TeV at the LHC and $(3.9-9.3)$ TeV at the 100 TeV pp collider. We find that the sensitivities to the coefficients of $\mathcal{O}_{G-}$, $\widetilde{\mathcal{O}}_{G-}$ and $\hat{h}_{1,3}^\gamma$ are significantly higher than that of the case by assuming the on-shell $Z\gamma$ final states [1]. In addition, we have studied the perturbative unitarity constraints [22] on the nTGC contributions, as presented in Section S3 of the Supplemental Material [21]. We demonstrate [21] that the unitarity bounds on Λ_j and h_j^V are much weaker than our current collider bounds in Tables 1-2, hence they do not affect our collider analyses.

Finally, we analyze the correlation contours (95% C.L.) between the sensitivities to the form factors of the off-shell nTGC vertex $Z^*\gamma V^*$, as shown in Fig. 2, where we have chosen an ideal detection efficiency $\epsilon = 100\%$. We find that the behavior of the $\hat{h}_4 - \hat{h}_3^Z$ correlation is similar to that of their on-shell counterparts h_4 and h_3^Z [1]. Specifically, the $\hat{h}_4 - \hat{h}_3^V$ correlation is rather small, while the sensitivity to $\hat{h}_3^\gamma$ is much greater than that to h_{31}^γ, especially at a 100 TeV pp collider. On the other hand, the correlation between $\hat{h}_3^Z - \hat{h}_3^\gamma$ is large at the LHC, but almost invisible at the 100 TeV pp collider. This is because the $\hat{h}_3^\gamma$ contribution is enhanced by the off-shell momentum-square q_1^2/M_Z^2 of Z^* and $\hat{h}_3^Z$ is not, which make the $\hat{h}_3^Z - \hat{h}_3^\gamma$ correlation suppressed by $1/\sqrt{q_1^2}$. At the LHC the on-shell and off-shell contributions to h_3^γ are comparable and thus the $\hat{h}_3^Z - \hat{h}_3^\gamma$ correlation can be significant, whereas their correlation is much suppressed by $1/\sqrt{q_1^2}$ at the 100 TeV pp collider and thus becomes nearly invisible.

We note that no correlation exists between the CPC and CPV nTGCs because their amplitudes only differ by $\pm$i. Finally, correlations among $\hat{h}_2$, $\hat{h}_1^Z$, $\hat{h}_1^\gamma$, and h_{11}^γ are similar to those of the corresponding CPC nTGCs, because the squared term σ_2 dominates the signal cross section at the LHC and at the 100 TeV pp collider.

4. Conclusions

In this work, we have demonstrated that the reaction $pp(q\bar{q}) \to Z^*\gamma \to \nu\bar{\nu}\gamma$ can probe sensitively both the CPC and CPV nTGCs at the LHC and at the projected 100 TeV pp colliders. It has comparable sensitivities to the on-shell production channels $pp(q\bar{q}) \to Z\gamma$ with $Z \to \ell^+\ell^-$ [1]. Because the on-shell constraint cannot be imposed on the final state Z boson with invisible decays at hadron colliders, we studied the $Z^*\gamma$ production with off-shell decays $Z^* \to \nu\bar{\nu}$. For this, we presented a new general formulation of the CPC/CPV doubly off-shell $Z^*\gamma V^*$ form factors and their nontrivial matching with the full SU(2)⊗U(1) gauge-invariant SMEFT operators of dimension-8. In consequence, we found that the conventional on-shell form factors for $Z\gamma V^*$ vertices [7] are inadequate, and the conventional form factors (h_3^V, h_4^V) and (h_1^V, h_2^V) must be replaced by two sets of new form factors $(h_{31}^\gamma, \hat{h}_3^V, \hat{h}_4)$ and $(h_{11}^\gamma, \hat{h}_1^V, \hat{h}_2)$, as shown in

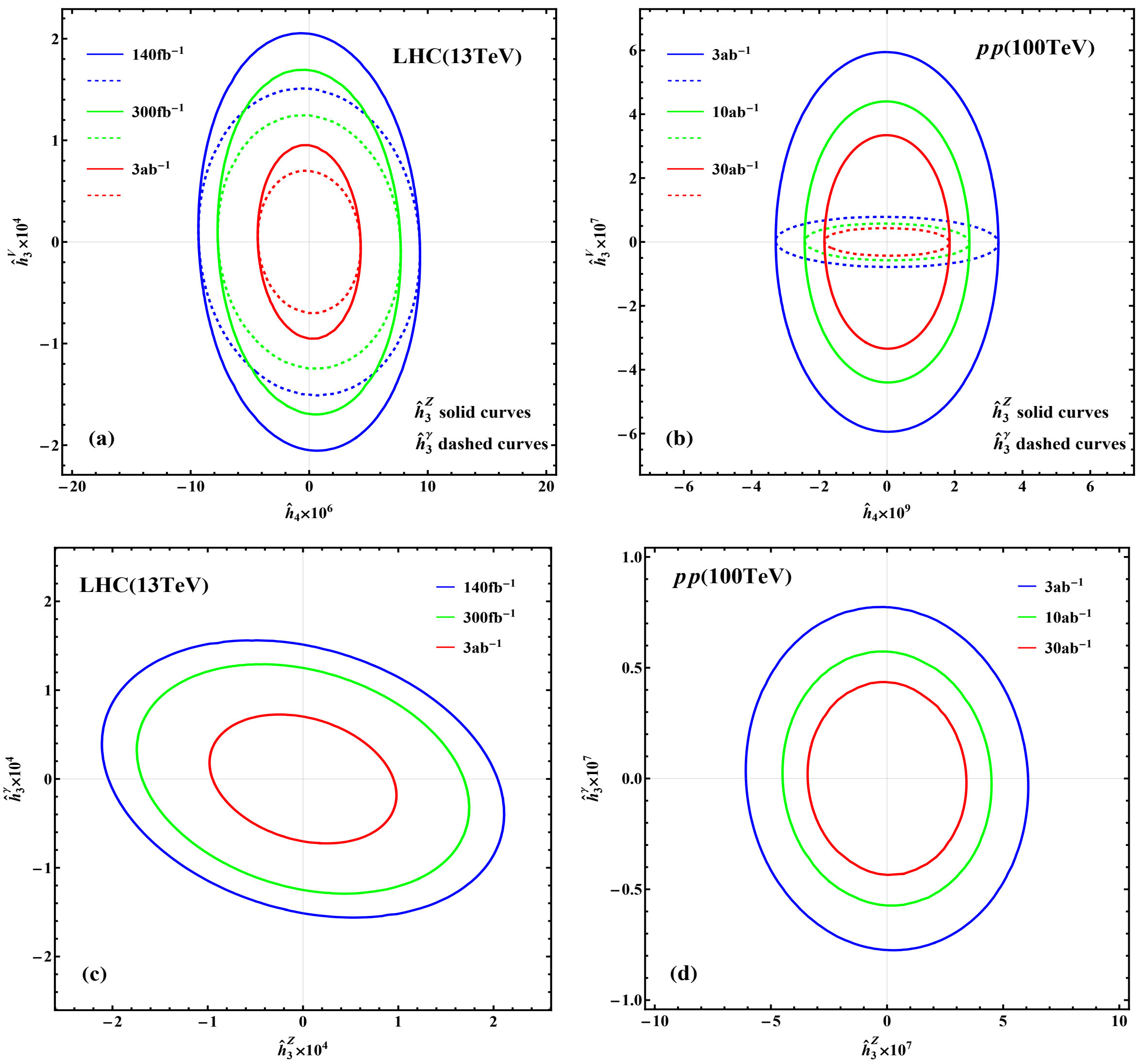

Figure 2: *Correlation contours* (95% C.L.) *for the sensitivities to each pairs of nTGC form factors at the* LHC (13 TeV) [panels (*a*) and (*c*)] *and the* 100 TeV *pp collider* [panels (*b*) and (*d*)]. Panels (a) and (b) *show the correlation contours for* $(h_4,\, h_3^Z)$ *(solid curves) and* $(h_4,\, h_3^\gamma)$ *(dashed curves), and* panels (c) and (d) *depict the correlation contours for* $(h_3^Z,\, h_3^\gamma)$.

Eqs.(2.5) and (2.7).

In the $\nu\bar{\nu}\gamma$ production channel at pp colliders, only the photon P_T^γ is measurable, and we have studied how to optimize the sensitivities to nTGCs by proper choices of P_T^γ bins at the LHC and the projected 100 TeV pp colliders. Since the interference cross section is always negligible relative to the squared term at these colliders [17], the sensitivities to the CPV nTGCs are similar to those to the corresponding CPC nTGCs.

We have presented the prospective sensitivity reaches on the nTGC form factors $\hat{h}_j^V$ (compatible with the full electroweak gauge symmtry with spontaneous breaking) at the LHC and the 100 TeV pp collider in Table 1, and the sensitivity reaches on probing the new physics scales Λ_j of the corresponding dimension-8 nTGC operators in Table 2. We found in Table 1 that including the off-shell decays $Z^*\!\to\nu\bar{\nu}$ can increase the sensitivity reaches for $(\hat{h}_3^\gamma,\, \hat{h}_1^\gamma)$ by (50–60)% at the LHC and by a factor of $O(10)$ at the 100 TeV pp collider. We present in Fig. 2

the correlations between the sensitivities to each pair of nTGC form factors.

We further made quantitative comparisons between the existing ATLAS measurements [5] of the CPC nTGC form factors and our new predictions, as shown in Eqs.(3.5)-(3.6). We found that for the $\nu\bar{\nu}\gamma$ channel the LHC sensitivity reaches on probing the nTGC form factors $\hat{h}_3^\gamma$ and $\hat{h}_4$ differ significantly from the ATLAS results (using the conventional $Z\gamma V^*$ formulae which are inconsistent with spontaneous breaking of the electroweak gauge symmetry).

This work establishes a new perspective for on-going experimental probes of the new physics in nTGCs at the LHC and the projected 100 TeV pp colliders. We look forward to continuing the fruitful cooperation with the LHC experimental groups, extending their on-going nTGC analyses by using our new nTGC formulation, which consistently incorporates the nTGC form factors with the corresponding gauge-invariant dimension-8 operators of the SMEFT.

Acknowledgements

The work of JE was supported in part by United Kingdom STFC Grant ST/T000759/1, and in part by the SJTU distinguished visiting fellow programme. The work of HJH and RQX was supported in part by the National NSF of China (under grants 11835005 and 12175136). RQX has been supported by an International Postdoctoral Exchange Fellowship.

References

[1] J. Ellis, H.-J. He, R.-Q. Xiao, Phys. Rev. D 107 (2023) 035005, no.3, [arXiv:2206.11676].

[2] J. Ellis, H.-J. He, and R.-Q. Xiao, Science China (Phys. Mech. Astron.) 64 (2021) 221062, no.2, [arXiv:2008.04298].

[3] J. Ellis, S.-f. Ge, H.-J. He, and R.-Q. Xiao, Chin. Phys. C 44 (2020) 063106, no.6, [arXiv: 1902.06631].

[4] V. Khachatryan *et al.* [CMS Collaboration], Phys. Lett. B 760 (2016) 448-468 [arXiv: 1602.07152 [hep-ex]].

[5] M. Aaboud *et al.* [ATLAS Collaboration], JHEP 12 (2018) 010 [arXiv:1810.04995 [hep-ex]].

[6] E.g., S. Jahedi, arXiv:2305.11266 [hep-ph]; S. Spor, E. Gurkanli and M. Köksal, arXiv: 2302.08245 [hep-ph]; S. Jahedi and J. Lahiri, JHEP 04 (2023) 085 [arXiv:2212.05121 [hep-ph]]; S. Spor, Nucl. Phys. B 991 (2023) 116198 [arXiv:2207.11585 [hep-ph]]; A. Senol, S. Spor, E. Gurkanli, V. Cetinkaya, H. Denizli, and M. Köksal, Eur. Phys. J. Plus 137 (2022) 1354, no.12 [arXiv:2205.02912 [hep-ph]]; Q. Fu, J. C. Yang, C. X. Yue, and Y. C. Guo, Nucl. Phys. B 972 (2021) 115543 [arXiv:2102.03623 [hep-ph]]. A. Biekötter, P. Gregg, F. Krauss, and M. Schönherr, Phys. Lett. B 817 (2021) 136311 [arXiv:2102.01115 [hep-ph]]; A. Senol, H. Denizli, A. Yilmaz, I. Turk Cakir, K. Y. Oyulmaz, O. Karadeniz, and O. Cakir, Nucl. Phys. B 935 (2018) 365 [arXiv:1805.03475 [hep-ph]]; R. Rahaman and R. K. Singh, Eur. Phys. J. C 77 (2017) 521, no.8 [arXiv:1703.06437 [hep-ph]]; Eur. Phys. J. C 76 (2016) 539, no.10 [arXiv:1604.06677 [hep-ph]].

[7] G. J. Gounaris, J. Layssac, and F. M. Renard, Phys. Rev. D 61 (2000) 073013 [arXiv:hep-ph/9910395]; Phys. Rev. D 62 (2000) 073012; D 65 (2002) 017302 [arXiv:hep-ph/0005269].

[8] C. Degrande, JHEP 1402 (2014) 101 [arXiv:1308.6323 [hep-ph]].

[9] H.-L. Li, Z. Ren, J. Shu, M.-L. Xiao, J.-H. Yu and Y.-H. Zheng, Phys. Rev. D 104 (2021) 015026, no.1, [arXiv:2005.00008 [hep-ph]]; C. W. Murphy, JHEP 10 (2020) 174 [arXiv:2005.00059 [hep-ph]].

[10] For reviews, see John Ellis, arXiv:2105.14942 [hep-ph], in the conference proceedings of "Beyond Standard Model: From Theory to Experiment" (BSM-2021), Zewail City, Egypt, March 29-31, 2021; I. Brivio and M. Trott, Phys. Rept. 793 (2019) 1 [arXiv:1706.08945 [hep-ph]].

[11] B. Grzadkowski, M. Iskrzynski, M. Misiak, and J. Rosiek, JHEP 10 (2010) 085 [arXiv: 1008.4884 [hep-ph]]; and references therein.

[12] See, e.g., J. Ellis, V. Sanz, and T. You, JHEP 1407 (2014) 036 [Xiv:1404.3667 [hep-ph]] and JHEP 1503 (2015) 157 [arXiv:1410.7703 [hep-ph]]; H.-J. He, J. Ren, and W. Yao, Phys. Rev. D 93 (2016) 015003 [arXiv:1506.03302 [hep-ph]]; J. Ellis and T. You, JHEP 03 (2016) 089 [arXiv:1510.04561 [hep-ph]; S.-F. Ge, H.-J. He, and R.-Q. Xiao, JHEP 10 (2016) 007 [arXiv:1603.03385]; J. de Blas et al., JHEP 12 (2016) 135 [arXiv:1608.01509 [hep-ph]]; F. Ferreira, B. Fuks, V. Sanz, and D. Sengupta, Eur. Phys. J. C 77 (2017) 675 [arXiv:1612.01808 [hep-ph]]; J. Ellis, P. Roloff, V. Sanz, and T. You, JHEP 05 (2017) 096 [arXiv:1701.04804 [hep-ph]]; G. Durieux, C. Grojean, J. Gu and K. Wang, JHEP 09 (2017) 014 [arXiv:1704.02333 [hep-ph]]; T. Barklow et al., Phys. Rev. D 97 (2018) 053003 [arXiv:1708.08912 [hep-ph]]; C. W. Murphy, Phys. Rev. D 97 (2018) 015007 [arXiv:1710.02008 [hep-ph]]; J. Ellis, C. W. Murphy, V. Sanz, and T. You, JHEP 06 (2018) 146 [arXiv:1803.03252]; G. N. Remmen and N. L. Rodd, JHEP 12 (2019) 032 [arXiv:1908.09845 [hep-ph]]; A. Gutierrez-Rodriguez, M. Koksal, A. A. Billur, M. A. Hernandez-Ruiz, J. Phys. G 47 (2020) 055005 [arXiv:1910.02307 [hep-ph]]; M. Koksal, A. A. Billur, A. Gutierrez-Rodriguez, and M. A. Hernandez-Ruiz, Phys. Lett. B 808 (2020) 135661 [arXiv:1910.06747 [hep-ph]]; J. Ellis, M. Madigan, K. Mimasu, V. Sanz, and T. You, JHEP 04 (2021) 279 [arXiv:2012.02779 [hep-ph]]. and references therein.

[13] We emphasize that the conventional electroweak form factor formulation imposes only the U(1) gauge symmetry of QED, and is in general *incompatible* with the SMEFT framework, which takes into account the full SU(2)⊗U(1) electroweak gauge symmetry of the SM. We stress that it is important to match precisely the form factors with the corresponding SMEFT operators in the broken phase, which can place additional nontrivial constraints on the structure of the form factors as a result of the spontaneous electroweak symmetry breaking of the SM. We demonstrate this for our correct formulation of the nTGC form factors in Section 3.

[14] We note that the CMS [4] and ATLAS [5] collaborations also measured the CPC nTGC form factor h_4^V using the conventional formula, which gives rise to unphysically large high-energy behavior [1].

[15] For a comprehensive review, see H. J. He, Y. P. Kuang and C. P. Yuan, arXiv:hep-ph/9704276 and DESY-97-056, in the Proceedings of the Workshop on "Physics at the TeV Energy Scale", vol.72 (1996), p.119. See also, H. J. He and W. B. Kilgore, Phys. Rev. D 55 (1997) 1515; H. J. He, Y. P. Kuang and C. P. Yuan, Phys. Rev. D 51 (1995) 6463; Phys.

Rev. D 55 (1997) 3038; H. J. He, Y. P. Kuang and X. Li, Phys. Lett. B 329 (1994) 278; Phys. Rev. D 49 (1994) 4842; Phys. Rev. Lett. 69 (1992) 2619; and references therein.

[16] H. L. Lai *et al.* [CTEQ Collaboration], Eur. Phys. J. C 12 (2000) 375-392 [hep-ph/9903282 [hep-ph]]; T. J. Hou *et al.* [CTEQ Collaboration], Phys. Rev. D 103 (2021) 014013, no.1 [1912.10053 [hep-ph]].

[17] We find that the situation is different for probing the nTGCs at high-energy e^+e^- colliders [2][3][18], where the interference contribution can dominate over the squared contribution.

[18] J. Ellis, H.-J. He, and R.-Q. Xiao, in preparation.

[19] We thank our ATLAS colleague Shu Li for discussing the ATLAS analyses and the estimate of their detection efficiency.

[20] G. Cowan, K. Cranmer, E. Gross, and O. Vitells, Eur. Phys. J. C 71 (2011) 1554 [arXiv:1007.1727 [physics.data-an]].

[21] J. Ellis, H.-J. He, R.-Q. Xiao, Supplemental Material.

[22] D. A. Dicus and H.-J. He, Phys. Rev. D 71 (2005) 093009 [arXiv:hep-ph/0409131]; and Phys. Rev. Lett. 94 (2005) 221802 [arXiv:hep-ph/0502178].

Probing Neutral Triple Gauge Couplings with $Z^*\gamma(\nu\bar{\nu}\gamma)$ Production at Hadron Colliders — Supplemental Material —

John Ellis [a], **Hong-Jian He** [b], **Rui-Qing Xiao** [c]

[a] Department of Physics, King's College London, Strand, London WC2R 2LS, UK;
Theoretical Physics Department, CERN, CH-1211 Geneva 23, Switzerland;
T. D. Lee Institute, Shanghai Jiao Tong University, Shanghai, China

[b] T. D. Lee Institute and School of Physics & Astronomy,
Key Laboratory for Particle Astrophysics and Cosmology,
Shanghai Key Laboratory for Particle Physics and Cosmology,
Shanghai Jiao Tong University, Shanghai, China;
Physics Department & Institute of Modern Physics, Tsinghua University, Beijing, China;
Center for High Energy Physics, Peking University, Beijing, China

[c] Department of Physics, King's College London, Strand, London WC2R 2LS, UK;
T. D. Lee Institute and School of Physics & Astronomy,
Shanghai Jiao Tong University, Shanghai, China

(john.ellis@cern.ch, hjhe@sjtu.edu.cn, xiaoruiqing@sjtu.edu.cn)

In this Supplemental Material, we provide further details to support the analyses in the main text[1]. These include three parts. In Section S1, we first derive systematically the neutral triple gauge boson vertices (nTGVs) at the Lagrangian level from the corresponding SU(2)⊗U(1) gauge-invariant dimension-8 operators of the SM Effective Field Theory (SMEFT) in its electroweak broken phase. Then, we present a systematic matching between the doubly off-shell $Z^*\gamma V^*$ form factors and the SMEFT operators, which puts nontrivial constraints on the neutral triple gauge coupling (nTGC) form factors and ensures the correct high energy behaviors. In Section S2, we provide cross section formulae for CP-conserving (CPC) and CP-violating (CPV) nTGC contributions to the reaction $q\bar{q}\to Z^*\gamma$. For comparison with the Tables I-II of the main text, we further present the combined sensitivitiy reaches on probing the nTGC form factors h_j^V and new physics scales Λ_j for both the $\nu\bar{\nu}\gamma$ channel[1] and $\ell^-\ell^+\gamma$ channel [1]. Finally, in Section S3, we present systematically the inelastic unitarity bounds on the nTGC form factors h_j^V and new physics scales Λ_j for both the CPC and CPV cases. These perturbative unitarity bounds are shown to be much weaker than our collider sensitivity reaches for the relevant energy scales, so they do not affect our present collider analyses.

S1. Matching $Z^*\gamma V^*$ Form Factors to the SMEFT Operators

For the present nTGC study, we have considered two classes of dimension-8 operators, $F^2H^2D^2$ and F^3D^2, where the symbols (F, H, D) denote the gauge field strength, Higgs doublet, and covariant derivative, respectively. Using integration by parts and equation of motion, F^3D^2

[1] J. Ellis, H.-J. He, R.-Q. Xiao, Phys. Rev. D (Letter) 108 (2023) L111704, no.11 [arXiv:2308.16887].

can be converted to operators of the forms F^4, $F^2\psi^2 D$, and $F^2H^2D^2$, where ψ denotes fermion field, and the classes of F^4 and $F^2\psi^2 D$ have no direct contribution to nTGCs. The operator type F^3D^2 was not chosen as the basis in Ref. [9] since its general classification [9] was not optimized for studying any specific type of new physics operators such as the nTGCs. We note that the operator class $F^2H^2D^2$ can contribute only to the form factors h_1^V and h_3^V, but not to the form factors h_2 and h_4. Thus, we find that without including the class F^3D^2, there would be no corresponding operators contributing to the form factors h_2 and h_4. Hence, choosing the operator basis of $F^2H^2D^2$ and F^3D^2 is necessary for a complete formulation of nTGCs and their phenomenological studies. As we have verified [1][2], for the reaction $f\bar{f} \to Z\gamma$, the contributions of $h_{2,4}$ from the F^3D^2 type operators are equivalent to that of certain combinations of $F^2H^2D^2$ and $F^2\psi^2 D$ operators. We studied [1][2] the fermionic operators of type $F^2\psi^2 D$:

$$\mathcal{O}_{C+} = \widetilde{B}_{\mu\nu}W^{a\mu\rho}\left[D_\rho(\overline{\psi_L}T^a\gamma^\nu\psi_L) + D^\nu(\overline{\psi_L}T^a\gamma_\rho\psi_L)\right], \tag{S1a}$$

$$\mathcal{O}_{C-} = \widetilde{B}_{\mu\nu}W^{a\mu\rho}\left[D_\rho(\overline{\psi_L}T^a\gamma^\nu\psi_L) - D^\nu(\overline{\psi_L}T^a\gamma_\rho\psi_L)\right]. \tag{S1b}$$

They are connected to nTGC operators by equation of motions,

$$\mathcal{O}_{C+} = \mathcal{O}_{G-} - \mathcal{O}_{\widetilde{B}W}\,, \tag{S2a}$$

$$\mathcal{O}_{C-} = \mathcal{O}_{G+} - \left\{\mathrm{i}H^\dagger \widetilde{B}_{\mu\nu}W^{\mu\rho}\left[D_\rho, D^\nu\right]H + \mathrm{i}\,2(D_\rho H)^\dagger \widetilde{B}_{\mu\nu}W^{\mu\rho}D^\nu H + \mathrm{h.c.}\right\}, \tag{S2b}$$

but they do not contribute directly to the nTGCs.

Working in the electroweak broken phase of the SM, $\mathrm{SU}(2)_W\otimes\mathrm{U}(1)_Y \to \mathrm{U}(1)_{\mathrm{em}}$, we expand the CPC operators and derive the relevant neutral triple gauge vertices (nTGVs) as follows:

$$\mathcal{O}_{G+}(\mathrm{CPC}) \to \frac{ev^2}{4M_Z^2 s_W c_W}\left(c_W^2\widetilde{A}_{\mu\nu}Z^{\mu\rho} - s_W^2\widetilde{Z}_{\mu\nu}A^{\mu\rho} + c_W s_W\widetilde{A}_{\mu\nu}A^{\mu\rho} - c_W s_W\widetilde{Z}_{\mu\nu}Z^{\mu\rho}\right)\partial^2\left(Z^\nu{}_\rho + \frac{s_W}{c_W}A^\nu{}_\rho\right), \tag{S3a}$$

$$\begin{aligned}\mathcal{O}_{G-}(\mathrm{CPC}) \to & -\frac{ev^2}{4M_Z^2 s_W c_W}\left(c_W^2\widetilde{A}_{\mu\nu}Z^{\mu\rho} - s_W^2\widetilde{Z}_{\mu\nu}A^{\mu\rho} + c_W s_W\widetilde{A}_{\mu\nu}A^{\mu\rho} - c_W s_W\widetilde{Z}_{\mu\nu}Z^{\mu\rho}\right) \\ & \times\left[\partial^2\left(\partial^\nu Z_\rho + \partial_\rho Z^\nu + \frac{s_W}{c_W}\partial^\nu A_\rho + \frac{s_W}{c_W}\partial_\rho A^\nu\right) - 2\partial^\nu\partial_\rho\left(\partial_\alpha Z^\alpha + \frac{s_W}{c_W}\partial_\alpha A^\alpha\right)\right],\end{aligned} \tag{S3b}$$

$$\mathcal{O}_{\widetilde{B}W}(\mathrm{CPC}) \to \frac{ev^2}{4s_W c_W}\left(c_W^2\widetilde{A}_{\mu\nu}Z^{\mu\rho} - s_W^2\widetilde{Z}_{\mu\nu}A^{\mu\rho} + c_W s_W\widetilde{A}_{\mu\nu}A^{\mu\rho} - c_W s_W\widetilde{Z}_{\mu\nu}Z^{\mu\rho}\right)\left(\partial^\nu Z_\rho + \partial_\rho Z^\nu\right), \tag{S3c}$$

$$\mathcal{O}_{\widetilde{BW}}(\mathrm{CPC}) \to \frac{-ev^2}{2s_W c_W}\left(\partial_\rho\widetilde{Z}_{\mu\nu}Z^{\mu\rho} + \partial_\rho\widetilde{A}_{\mu\nu}A^{\mu\rho}\right)Z^\nu\,, \tag{S3d}$$

where we adopt the notations $\widetilde{V}^{\mu\nu} = \epsilon^{\mu\nu\alpha\beta}V_{\alpha\beta}$ and $V^{\mu\nu} = \partial^\mu V^\nu - \partial^\nu V^\mu$ with $V = A, Z$.

We then expand the CPV operators in the electroweak broken phase respecting only the residual SM gauge symmetry $\mathrm{SU}(3)_C\otimes\mathrm{U}(1)_{\mathrm{em}}$. In this way we derive the relevant CPV nTGVs as follows:

$$\widetilde{\mathcal{O}}_{G+}(\mathrm{CPV}) \to \frac{ev^2}{4M_Z^2 s_W c_W}A_{\mu\nu}Z^{\mu\rho}\partial^2\left(Z^\nu{}_\rho + \frac{s_W}{c_W}A^\nu{}_\rho\right), \tag{S4a}$$

$$\begin{aligned}\widetilde{\mathcal{O}}_{G-}(\mathrm{CPV}) \to & -\frac{ev^2}{4M_Z^2 s_W c_W}\left[c_{2W}\left(A_{\mu\nu}Z^{\mu\rho} + Z_{\mu\nu}A^{\mu\rho}\right) + s_{2W}\left(A_{\mu\nu}A^{\mu\rho} - Z_{\mu\nu}Z^{\mu\rho}\right)\right] \\ & \times\left[\partial^2\left(\partial^\nu Z_\rho + \frac{s_W}{c_W}\partial^\nu A_\rho\right) - \partial^\nu\partial_\rho\left(\partial\cdot Z + \frac{s_W}{c_W}\partial\cdot A\right)\right],\end{aligned} \tag{S4b}$$

$$\widetilde{\mathcal{O}}_{BW}(\text{CPV}) \;\rightarrow\; \frac{ev^2}{4s_Wc_W}\big[c_{2W}\big(A_{\mu\nu}Z^{\mu\rho}+Z_{\mu\nu}A^{\mu\rho}\big)+s_{2W}\big(A_{\mu\nu}A^{\mu\rho}-Z_{\mu\nu}Z^{\mu\rho}\big)\big]\partial^\nu Z_\rho\,, \tag{S4c}$$

$$\widetilde{\mathcal{O}}_{WW}(\text{CPV}) \;\rightarrow\; -\frac{ev^2}{4s_Wc_W}\,\big[s_Wc_W\big(A_{\mu\nu}Z^{\mu\rho}+Z_{\mu\nu}A^{\mu\rho}\big)+s_W^2A_{\mu\nu}A^{\mu\rho}+c_W^2Z_{\mu\nu}Z^{\mu\rho}\big]\partial^\nu Z_\rho\,, \tag{S4d}$$

$$\widetilde{\mathcal{O}}_{BB}(\text{CPV}) \;\rightarrow\; -ev^2\Big[-\big(A_{\mu\nu}Z^{\mu\rho}+Z_{\mu\nu}A^{\mu\rho}\big)+\frac{c_W}{s_W}A_{\mu\nu}A^{\mu\rho}+\frac{s_W}{c_W}Z_{\mu\nu}Z^{\mu\rho}\Big]\partial^\nu Z_\rho\,, \tag{S4e}$$

where we have defined $(s_{2W},\, c_{2W})\equiv(\sin 2\theta_W,\, \cos 2\theta_W)$. We note that in Eq.(S4b) the factor $\partial\!\cdot\! Z$ vanishes for an on-shell Z boson, while for an off-shell Z^* it also leads to vanishing results as long as the vector boson couples to a pair of fermions or gauge bosons with equal mass. The same is true for the factor $\partial\cdot A$. Thus, we can drop terms with either $\partial\cdot Z$ or $\partial\cdot A$ for the present study.

Our next step is to classify the *complete structure* of the nTGVs in the broken electroweak phase that are generated by the above SMEFT operators of dimension-8. The Lagrangian of these nTGVs in the electroweak broken phase contains the following CPC and CPV nTGC form factors, which generally hold for all fields being off-shell:

$$\begin{aligned}
\mathcal{L}_{\text{nTGC}}^{\text{CPC}} = {} & \frac{e\hat{h}_3^Z}{2M_Z^2}\big(c_W^2\widetilde{A}_{\mu\nu}Z^{\mu\rho}-s_W^2\widetilde{Z}_{\mu\nu}A^{\mu\rho}+c_Ws_W\widetilde{A}_{\mu\nu}A^{\mu\rho}-c_Ws_W\widetilde{Z}_{\mu\nu}Z^{\mu\rho}\big)\big(\partial^\nu Z_\rho+\partial_\rho Z^\nu\big) \\
& -\frac{e\hat{h}_4}{2M_Z^4}\big(c_W^2\widetilde{A}_{\mu\nu}Z^{\mu\rho}-s_W^2\widetilde{Z}_{\mu\nu}A^{\mu\rho}+c_Ws_W\widetilde{A}_{\mu\nu}A^{\mu\rho}-c_Ws_W\widetilde{Z}_{\mu\nu}Z^{\mu\rho}\big)\partial^2\Big({Z^\nu}_\rho+\frac{s_W}{c_W}{A^\nu}_\rho\Big) \\
& +\frac{ec_W\hat{h}_3^\gamma}{2s_WM_Z^4}\big(c_W^2\widetilde{A}_{\mu\nu}Z^{\mu\rho}-s_W^2\widetilde{Z}_{\mu\nu}A^{\mu\rho}+c_Ws_W\widetilde{A}_{\mu\nu}A^{\mu\rho}-c_Ws_W\widetilde{Z}_{\mu\nu}Z^{\mu\rho}\big)\times \\
& \quad \Big[\partial^2\Big(\partial^\nu Z_\rho+\partial_\rho Z^\nu+\frac{s_W}{c_W}\partial^\nu A_\rho+\frac{s_W}{c_W}\partial_\rho A^\nu\Big)-2\partial^\nu\partial_\rho\Big(\partial\cdot Z+\frac{s_W}{c_W}\partial\cdot A\Big)\Big] \\
& +\frac{eh_{31}^\gamma}{2M_Z^2}\big(\partial_\rho\widetilde{Z}_{\mu\nu}Z^{\mu\rho}+\partial_\rho\widetilde{A}_{\mu\nu}A^{\mu\rho}\big)Z^\nu ,
\end{aligned} \tag{S5a}$$

$$\begin{aligned}
\mathcal{L}_{\text{nTGC}}^{\text{CPV}} = {} & \frac{e\hat{h}_1^Z}{M_Z^2}\big(A_{\mu\nu}Z^{\mu\rho}+Z_{\mu\nu}A^{\mu\rho}\big)\partial^\nu Z_\rho+\frac{eh_{11}^\gamma}{M_Z^2}A_{\mu\nu}A^{\mu\rho}\partial^\nu Z_\rho-\frac{e\hat{h}_2}{2M_Z^4}A_{\mu\nu}Z^{\mu\rho}\partial^2\Big({Z^\nu}_\rho+\frac{s_W}{c_W}{A^\nu}_\rho\Big) \\
& -\frac{e\hat{h}_1^\gamma}{M_Z^4}\Big[c_{2W}\big(A_{\mu\nu}Z^{\mu\rho}+Z_{\mu\nu}A^{\mu\rho}\big)+s_{2W}\big(A_{\mu\nu}A^{\mu\rho}-Z_{\mu\nu}Z^{\mu\rho}\big)\Big] \\
& \quad\times\Big[\partial^2\partial^\nu\Big(\frac{c_W}{s_W}Z_\rho+A_\rho\Big)-\partial^\nu\partial_\rho\partial\cdot\Big(\frac{c_W}{s_W}Z+A\Big)\Big].
\end{aligned} \tag{S5b}$$

Matching the above form factor Lagrangian with the corresponding dimension-8 nTGC operators in Eq.(S4), we derive the following relations for the CPC nTGC form factors:

$$\hat{h}_4 = \frac{\hat{r}_4}{[\Lambda_{G+}^4]}\,, \qquad \hat{h}_3^Z = \frac{\hat{r}_3^Z}{[\Lambda_{\widetilde{B}W}^4]}, \qquad \hat{h}_3^\gamma = \frac{\hat{r}_3^\gamma}{[\Lambda_{G-}^4]}\,, \qquad h_{31}^\gamma = \frac{r_{31}^\gamma}{[\Lambda_{\widetilde{BW}}^4]}\,, \tag{S6a}$$

$$\hat{r}_4 = -\frac{v^2M_Z^2}{s_Wc_W}, \qquad \hat{r}_3^Z = \frac{v^2M_Z^2}{2s_Wc_W}\,, \qquad \hat{r}_3^\gamma = -\frac{v^2M_Z^2}{2c_W^2}\,, \qquad r_{31}^\gamma = -\frac{v^2M_Z^2}{s_Wc_W}\,, \tag{S6b}$$

and for the CPV form factors:

$$\hat{h}_1^Z \;=\; v^2M_Z^2\Big(-\frac{1}{4[\Lambda_{WW}^4]}+\frac{c_W^2-s_W^2}{4c_Ws_W[\Lambda_{WB}^4]}+\frac{1}{[\Lambda_{BB}^4]}\Big)\,, \tag{S7a}$$

$$h_{11}^\gamma \;=\; v^2M_Z^2\Big(-\frac{s_W}{4c_W[\Lambda_{WW}^4]}+\frac{1}{2[\Lambda_{WB}^4]}-\frac{c_W}{s_W[\Lambda_{BB}^4]}\Big)\,, \tag{S7b}$$

$$\hat{h}_1^{\gamma} = \frac{v^2 M_Z^2}{4c_W^2[\Lambda_{\widetilde{G}-}^4]}\,, \tag{S7c}$$

$$\hat{h}_2 = -\frac{v^2 M_Z^2}{2s_W c_W[\Lambda_{\widetilde{G}+}^4]}\,, \tag{S7d}$$

where $[\Lambda_j^4] \equiv \text{sign}(\tilde{c}_j)\Lambda_j^4$. We stress that the nTGC form factor formulas in Eq.(S5) generally hold at the Lagrangian level *with all the fields being off-shell,* and they are consistently built upon the SMEFT broken phase formulation of the nTGCs. This provides a fully general and consistent off-shell formulation of nTGCs at the Lagrangian level.

Next, using the general Lagrangian formulation of nTGVs in Eq.(S5), we further derive the neutral triple gauge vertices $Z^*\gamma V^*$ by requiring one photon field A^μ be on-shell, where the on-shell photon field satisfies the conditions $\partial^2 A^\mu = 0$ and $\partial_\mu A^\mu = 0$. Thus, we can derive the complete form factor formulation of the doubly off-shell nTGVs in momentum space:

$$V_{Z^*\gamma V^*}^{\alpha\beta\mu} = \Gamma_{Z^*\gamma V^*}^{\alpha\beta\mu} + \frac{e}{M_Z^2} X_{1V}^{\beta\mu} q_1^\alpha + \frac{e}{M_Z^2} X_{3V}^{\alpha\beta} q_3^\mu\,, \tag{S8}$$

where the expressions of $X_{1V}^{\beta\mu}$ and $X_{3V}^{\alpha\beta}$ are given as follows:

$$X_{1V}^{\beta\mu} = \epsilon^{\beta\mu\nu\sigma} q_{2\nu} q_{3\sigma}\left(\chi_{10}^V + \chi_{11}^V \frac{q_1^2}{M_Z^2} + \chi_{13}^V \frac{q_3^2}{M_Z^2}\right) + (q_3^2 - q_1^2)\, g^{\beta\mu}\left(\tilde{\chi}_{10}^V + \tilde{\chi}_{11}^V \frac{q_1^2}{M_Z^2} + \tilde{\chi}_{13}^V \frac{q_3^2}{M_Z^2}\right), \tag{S9a}$$

$$X_{3V}^{\alpha\beta} = \epsilon^{\alpha\beta\nu\sigma} q_{2\nu} q_{3\sigma}\left(\chi_{30}^V + \chi_{31}^V \frac{q_1^2}{M_Z^2} + \chi_{33}^V \frac{q_3^2}{M_Z^2}\right) + (q_3^2 - q_1^2)\, g^{\alpha\beta}\left(\tilde{\chi}_{30}^V + \tilde{\chi}_{31}^V \frac{q_1^2}{M_Z^2} + \tilde{\chi}_{33}^V \frac{q_3^2}{M_Z^2}\right). \tag{S9b}$$

In the above the additional form factor coefficients χ_{ij}^V are defined as follows:

$$\begin{aligned}
&\chi_{10}^Z = \frac{\eta_{\widetilde{B}W}}{t_W}, \quad \chi_{11}^Z = -\frac{\eta_{G+}}{2t_W} + \frac{t_W \eta_{G-}}{2}, \quad \chi_{30}^Z = \frac{\eta_{\widetilde{B}W}}{t_W}, \quad \chi_{31}^Z = \frac{\eta_{G+}}{2t_W} - \frac{t_W \eta_{G-}}{2},\\
&\chi_{10}^\gamma = \frac{\eta_{\widetilde{B}W}}{2}, \quad \chi_{11}^\gamma = -\frac{\eta_{G+}}{2} - \frac{\eta_{G-}}{2}, \quad \chi_{30}^\gamma = \frac{\eta_{\widetilde{B}W}}{2}, \quad \chi_{31}^\gamma = \frac{\eta_{G+}}{2} - \frac{t_W^2 \eta_{G-}}{2},\\
&\tilde{\chi}_{10}^Z = -\frac{\eta_{BW}}{2t_{2W}} + \frac{\eta_{WW}}{4} - \eta_{BB}, \quad \tilde{\chi}_{11}^Z = \frac{\eta_{\widetilde{G}+}}{4s_{2W}}, \quad \chi_{13}^Z = -\frac{\eta_{\widetilde{G}+}}{4s_{2W}},\\
&\tilde{\chi}_{30}^Z = \frac{\eta_{BW}}{2t_{2W}} - \frac{\eta_{WW}}{4} + \eta_{BB}, \quad \tilde{\chi}_{31}^Z = \frac{\eta_{\widetilde{G}+}}{4s_{2W}}, \quad \chi_{33}^Z = -\frac{\eta_{\widetilde{G}+}}{4s_{2W}},\\
&\tilde{\chi}_{10}^\gamma = -\frac{\eta_{BW}}{4} + \frac{t_W \eta_{WW}}{8} + \frac{\eta_{BB}}{2t_W}, \quad \tilde{\chi}_{11}^\gamma = \frac{\eta_{\widetilde{G}-}}{8c_W^2}, \quad \tilde{\chi}_{13}^\gamma = -\frac{\eta_{\widetilde{G}+}}{8c_W^2} - \frac{\eta_{\widetilde{G}-}}{8c_W^2},\\
&\tilde{\chi}_{30}^\gamma = \frac{\eta_{BW}}{4} - \frac{t_W \eta_{WW}}{8} - \frac{\eta_{BB}}{2t_W}, \quad \tilde{\chi}_{31}^\gamma = \frac{\eta_{\widetilde{G}-}}{8c_W^2}, \quad \tilde{\chi}_{33}^\gamma = -\frac{\eta_{\widetilde{G}+}}{8c_W^2} - \frac{\eta_{\widetilde{G}-}}{8c_W^2},
\end{aligned} \tag{S10}$$

where $\eta_j = v^2 M_Z^2/[\Lambda_j^4]$, $t_W = s_W/c_W$, $t_{2W} = s_{2W}/c_{2W}$, and $(s_{2W}, c_{2W}) = (\sin 2\theta_W, \cos 2\theta_W)$. Using the on-shell conditions for the initial/final state fermions, we can readily prove that the contributions of $X_{1V}^{\beta\mu}$ and $X_{3V}^{\alpha\beta}$ to the physical processes of the present study vanish, so they are not needed for this work, but we list them here for completeness.

Finally, we clarify the difference between our new nTGC form factor formulation and the conventional nTGC form factor formulation [7]. Since there is no conventional form factor formulation for the doubly off-shell nTGVs $Z^*\gamma V^*$ (with only γ on-shell) given in the literature [7][8], we compare our new formulation and the conventional formulation [7] for the nTGVs $Z\gamma V^*$ when both Z and γ are on-shell. The conventional form factor parametrization of the CPC and CPV neutral triple gauge vertices $\widetilde{\Gamma}^{\alpha\beta\mu}_{Z\gamma V^*}$ yield the following formulae [7]:

$$\widetilde{\Gamma}^{\alpha\beta\mu(\mathrm{CPC})}_{Z\gamma V^*} = \frac{e\,(q_3^2-M_V^2)}{M_Z^2}\left[h_3^V\, q_{2\nu}\epsilon^{\alpha\beta\mu\nu} + \frac{h_4^V}{M_Z^2}\, q_2^\alpha\, q_{3\nu}\, q_{2\sigma}\,\epsilon^{\beta\mu\nu\sigma}\right], \tag{S11a}$$

$$\widetilde{\Gamma}^{\alpha\beta\mu(\mathrm{CPV})}_{Z\gamma V^*} = \frac{e\,(q_3^2-M_V^2)}{M_Z^2}\left[h_1^V\,(q_2^\alpha g^{\mu\beta} - q_2^\mu g^{\alpha\beta}) + \frac{h_2^V}{2M_Z^2}\, q_2^\alpha g^{\mu\beta}(M_Z^2-q_3^2)\right]. \tag{S11b}$$

We found in [1] that the conventional CPC form factor h_4^V of Eq.(S11a) is incompatible with the spontaneous breaking of the full electroweak gauge group $\mathrm{SU(2)}_W\otimes\mathrm{U(1)}_Y\to\mathrm{U(1)}_{\mathrm{em}}$, and leads to unphysically large high-energy behaviors. Hence we must introduce a new form factor h_5^V as in Eq.(S12a) for matching consistently with the broken phase results originating from the CPC dimension-8 operators (2.2a)-(2.2b) and (2.3a)-(2.3b) of the SMEFT that respect the underlying electroweak $\mathrm{SU(2)}_W\otimes\mathrm{U(1)}_Y$ gauge symmetry. Furthermore, we find that the conventional CPV form factor h_2^V of Eq.(S11b) is incompatible with the spontaneous breaking of the full electroweak gauge group $\mathrm{SU(2)}_W\otimes\mathrm{U(1)}_Y\to\mathrm{U(1)}_{\mathrm{em}}$ and also causes unphysically large high-energy behavior. To construct a consistent formulation, we introduce another new form factor h_6^V as in Eq.(S12b) to match with the broken phase results originating from the CPV dimension-8 operators (2.2c)-(2.2e) and (2.3c)-(2.3d) of the SMEFT that respect the full underlying electroweak gauge symmetry. We then present the extended nTGC form factor formulations for both the CPC case [1] and the CPV case:

$$\Gamma^{\alpha\beta\mu(\mathrm{CPC})}_{Z\gamma V^*} = \frac{e\,(q_3^2-M_V^2)}{M_Z^2}\left[\left(h_3^V + h_5^V\frac{q_3^2}{M_Z^2}\right) q_{2\nu}\epsilon^{\alpha\beta\mu\nu} + \frac{h_4^V}{M_Z^2}\, q_2^\alpha\, q_{3\nu}\, q_{2\sigma}\,\epsilon^{\beta\mu\nu\sigma}\right], \tag{S12a}$$

$$\begin{aligned}\Gamma^{\alpha\beta\mu(\mathrm{CPV})}_{Z\gamma V^*} &= \frac{e\,(q_3^2-M_V^2)}{M_Z^2}\left[\left(h_1^V + h_6^V\frac{q_3^2}{M_Z^2}\right)(q_2^\alpha g^{\mu\beta} - q_2^\mu g^{\alpha\beta}) + \frac{h_2^V}{2M_Z^2}\, q_2^\alpha g^{\mu\beta}(M_Z^2-q_3^2)\right] \\ &= \frac{e\,(q_3^2-M_V^2)}{M_Z^2}\left[h_1^V(q_2^\alpha g^{\mu\beta} - q_2^\mu g^{\alpha\beta}) + \frac{h_2^V M_Z^2 q_2^\alpha g^{\mu\beta} - 2h_6^V q_3^2 q_2^\mu g^{\alpha\beta}}{2M_Z^2} + \frac{2h_6^V - h_2^V}{2M_Z^2} q_3^2 q_2^\alpha g^{\mu\beta}\right],\end{aligned} \tag{S12b}$$

where the form factor coefficients $h_{1,2,3,4}^V$ are the conventional form factors [7] and the form factor terms $\propto h_5^V$ and h_6^V belong to our extension. We observe that the form factor coefficients $(h_4^V,\, h_5^V)$ (CPC) and $(h_2^V,\, h_6^V)$ (CPV) are subject to further constraints due to the matching with the broken phase results of the corresponding dimension-8 nTGC operators that respect the full $\mathrm{SU(2)}_W\otimes\mathrm{U(1)}_Y$ electroweak gauge symmetry. These constraints ensure that for each scattering amplitude the nTGC form factor contributions have the same high-energy behaviors as those of the corresponding dimension-8 nTGC operators. For this, we make a precise matching between the above nTGC form factor formulae (S12a)-(S12b) and the dimension-8 nTGC operators (2.2)-(2.3). From these we derive the following nontrivial relations between the nTGC form factor coefficients:

$$h_4^V = 2h_5^V\,, \qquad h_2^V = 2h_6^V\,, \tag{S13a}$$

$$h_4^Z = \frac{c_W}{s_W}h_4^\gamma\,, \quad h_2^Z = \frac{c_W}{s_W}h_2^\gamma\,. \tag{S13b}$$

Imposing these relations, we can further express the formulae (S12a) and (S12b) as follows:

$$\Gamma^{\alpha\beta\mu(\mathrm{CPC})}_{Z\gamma V^*} = \frac{e\,(q_3^2-M_V^2)}{M_Z^2}\left[\left(h_3^V + h_4^V\frac{q_3^2}{2M_Z^2}\right) q_{2\nu}\epsilon^{\alpha\beta\mu\nu} + \frac{h_4^V}{M_Z^2}\, q_2^\alpha\, q_{3\nu}\, q_{2\sigma}\,\epsilon^{\beta\mu\nu\sigma}\right], \tag{S14a}$$

$$\Gamma^{\alpha\beta\mu(\mathrm{CPV})}_{Z\gamma V^*} = \frac{e\,(q_3^2-M_V^2)}{M_Z^2}\left[h_1^V(q_2^\alpha g^{\mu\beta} - q_2^\mu g^{\alpha\beta}) + h_2^V\,\frac{M_Z^2 q_2^\alpha g^{\mu\beta} - q_3^2 q_2^\mu g^{\alpha\beta}}{2M_Z^2}\right]. \tag{S14b}$$

Applying naive power counting on the individual contributions of the nTGC form factors of Eqs.(S12a)-(S12b) to the scattering amplitude for $f\bar{f}\to Z\gamma$, we deduce the size of each individual contribution as follows:

$$\mathcal{T}[Z_T\gamma_T](\text{CPC}) = h_3^V O(E^2) + h_5^V O(E^4)\,, \tag{S15a}$$
$$\mathcal{T}[Z_L\gamma_T](\text{CPC}) = h_3^V O(E^3) + h_4^V O(E^5) + h_5^V O(E^5)\,, \tag{S15b}$$
$$\mathcal{T}[Z_T\gamma_T](\text{CPV}) = h_1^V O(E^2) + h_6^V O(E^4)\,, \tag{S15c}$$
$$\mathcal{T}[Z_L\gamma_T](\text{CPV}) = h_1^V O(E^3) + h_2^V O(E^5) + h_6^V O(E^5)\,. \tag{S15d}$$

We note that the form factors h_4^V and h_2^V do not contribute to the amplitudes with final state $Z_T\gamma_T$. This is because the h_4^V and h_2^V vertices in Eqs.(S12a)-(S12b) contain the momentum $q_2^\alpha = -(q_1^\alpha + q_3^\alpha)$, and thus the contraction $q_1^\alpha \epsilon^Z_{T\alpha}(q_1)$ vanishes due to the on-shell condition of Z boson, and the other contraction $q_3^\alpha \epsilon^Z_{T\alpha}(q_1)$ vanishes due to the fact that the s-channel momentum q_3^α has no spatial component and the transverse polarization vector $\epsilon^Z_{T\alpha}$ has no time component.

Inspecting the scattering amplitudes of Eq.(S15), we note that for the final state $Z_L\gamma_T$, the largest individual contributions of $\mathcal{O}(E^5)$ arise from the form factors (h_4^V, h_5^V) for the CPC case, as shown in Eq.(S15b), and from the form factors (h_2^V, h_6^V) for the CPV case as shown in Eq.(S15d). We have verified explicitly that upon imposing the matching constraints $h_4^V = 2h_5^V$ (CPC case) and $h_2^V = 2h_6^V$ (CPV case) of Eq.(S13a), the sum of the individual leading contributions exhibits an exact energy cancellation $O(E^5) \to O(E^3)$ for each amplitude. Thus, the nonzero leading contributions behave as $O(E^4)$ and arise from the final state $Z_T\gamma_T$ instead. The large energy cancellations $O(E^5) \to O(E^3)$ can be understood by applying the equivalence theorem (ET) [15] to the high-energy scattering process $f\bar{f} \to Z_L\gamma_T$. For $E \gg M_Z$, the ET gives:

$$\mathcal{T}[Z_L, \gamma_T] = \mathcal{T}[-\mathrm{i}\pi^0, \gamma_T] + B\,, \tag{S16}$$

where the longitudinal gauge boson Z_L absorbs the would-be Goldstone boson π^0 through the Higgs mechanism, and the residual term $B = \mathcal{T}[v^\mu Z_\mu, \gamma_T]$ is suppressed by the quantity $v^\mu \equiv \epsilon_L^\mu - q_Z^\mu/M_Z = O(M_Z/E_Z)$ [15]. We note that the ET (S16) cannot be directly applied to the conventional form factor formulation (S11), because it obeys only the gauge symmetry $\mathrm{U}(1)_{\text{em}}$ and does not respect the full electroweak gauge symmetry of the SM. More generally, the form factor formulation is normally given in the broken phase of the electroweak gauge symmetry and contains no would-be Goldstone boson. We should apply the ET to the electroweak gauge-invariant formulation of the nTGCs which can be derived only from the dimension-8 operators as in Eqs.(2.2)-(2.3). Thus, we can analyze the allowed leading energy-dependences of the amplitudes (S15b) and (S15d) by applying the ET to the contributions of the dimension-8 nTGC operators in Eqs. (2.2)-(2.3). From these, we find that only the Higgs-related nTGC operators in Eq.(2.2) could contribute to the Goldstone amplitude $\mathcal{T}[-\mathrm{i}\pi^0, \gamma_T]$ with a leading energy-dependence $O(E^3)$ that corresponds to the form factor h_3^Z or h_1^Z. The operators $\mathcal{O}_{G_\pm}$ or $\widetilde{\mathcal{O}}_{G_\pm}$ do not contribute to the Goldstone boson amplitude $\mathcal{T}[-\mathrm{i}\pi^0, \gamma_T]$, but they contribute the largest residual term $B = O(E^3)$. With these results, we apply the ET (S16) and deduce that in Eqs.(S15b) and (S15d) the individual leading terms of $O(E^5)$ due to the form factors (h_4^V, h_5^V) (CPC case) or (h_2^V, h_6^V) (CPV case) must exactly cancel with each other for the on-shell amplitude $\mathcal{T}[Z_L, \gamma_T]$, from which we derive the the following conditions:

$$h_4^V/h_5^V = 2\,, \qquad h_2^V/h_6^V = 2\,, \tag{S17}$$

in agreement with Eq.(S13a). From the above, we further conclude that the final nonzero leading amplitude is $O(E^4)$ as in $\mathcal{T}[Z_T\gamma_T]$ and is contributed by h_5^V for the CPC case shown in Eq.(S15a) or by h_6^V for the CPV case shown in Eq.(S15c).

Next we consider the scattering process $f\bar{f} \to Z^*\gamma \to f'\bar{f}'\gamma$ with an off-shell Z^*, as studied in the main text. Using our doubly off-shell nTGV formulase in Eqs.(5) and (7), we can count the leading energy-dependence for the contribution of each form factor as follows:

$$\mathcal{T}[f'\bar{f}'\gamma_T](\text{CPC}) = h_{31}^{\gamma} O(E^1) + \hat{h}_3^{\gamma} O(E^3) + \hat{h}_3^{Z} O(E^1) + \hat{h}_4 O(E^3)\,, \tag{S18a}$$

$$\mathcal{T}[f'\bar{f}'\gamma_T](\text{CPV}) = h_{11}^{\gamma} O(E^1) + \hat{h}_1^{\gamma} O(E^3) + \hat{h}_1^{Z} O(E^1) + \hat{h}_2 O(E^3)\,. \tag{S18b}$$

We see that the nonzero leading energy dependence is $O(E^3)$, contributed by the form factors $(\hat{h}_3^{\gamma},\, \hat{h}_4)$ and $(\hat{h}_1^{\gamma},\, \hat{h}_2)$. This is in contrast with the on-shell amplitudes $\mathcal{T}[Z_T\gamma_T]$ in Eqs.(S15a) and (S15c), which have nonzero leading energy-dependences of $O(E^4)$, contributed by h_5^V and h_6^V.

As shown in Eqs.(5) and (7) of Section II, we find that the contributions of $\hat{h}_3^{\gamma}$ and $\hat{h}_1^{\gamma}$ to the nTGVs are enhanced by a large factor q_1^2/M_Z^2 from the off-shell decays $Z^*(q_1)\!\to\nu\bar{\nu}\gamma$, whereas the contributions of $\hat{h}_{3,1}^{Z}$ and $\hat{h}_{4,2}$ are dominated by on-shell Z decays, so including off-shell Z^* decays does not cause significant changes in their sensitivity reaches. Hence, for studying the form factors $\hat{h}_4$ and $\hat{h}_2$, we can consider the $Z\gamma V^*$ nTGVs, and make a quantitative comparison between our new form factor formulation (S14) and the conventional form factor formulae (S11) [7] via the production channel $pp(q\bar{q})\to Z\gamma\to\nu\bar{\nu}\gamma$ at hadron colliders. We present this comparison in Table S3, where the third row (red color) depicts the sensitivity reaches on $\hat{h}_{4,2}$ obtained by using our nTGV formula (S14), and the last two rows (blue color) show the sensitivity reaches on $h_{4,2}^V$ that would be obtained by using the (incorrect) conventional nTGV formulas (S11) [7]. Table S3 demonstrates that the sensitivity reaches on the conventional nTGC form factors $h_{4,2}^V$ are erroneously stronger than those for our new formulation (S14) by about a factor of $O(20)$ at the LHC and by about a factor of $O(170)$ at a 100 TeV pp collider.

Finally, we comment on the possible variations of the operator structure $F^2H^2D^2$. We note that there are two subclasses of $F^2H^2D^2$ which can contribute to nTGCs [8]: $H^\dagger F_{\mu\nu}F^{\mu\rho}D_\rho D^\nu H$ and $H^\dagger D_\rho F_{\mu\nu}F^{\mu\rho}D^\nu H$. Using integration by parts, we can convert the operator $H^\dagger D_\rho F_{\mu\nu}F^{\mu\rho}D^\nu H$ to $H^\dagger F_{\mu\nu}F^{\mu\rho}D_\rho D^\nu H$ plus certain other operators. The operators of the subclass $H^\dagger F_{\mu\nu}F^{\mu\rho}D_\rho D^\nu H$ were shown in [8]. We further present the subclass $H^\dagger D_\rho F_{\mu\nu}F^{\mu\rho}D^\nu H$ which includes the following operators:

$$\begin{aligned}
\mathcal{O}_{BW}^{(1)} &= \mathrm{i}H^\dagger D_\rho \widetilde{B}_{\mu\nu}W^{\mu\rho}D^\nu H + \text{h.c.}, & \mathcal{O}_{WB}^{(1)} &= \mathrm{i}H^\dagger D_\rho \widetilde{W}_{\mu\nu}B^{\mu\rho}D^\nu H + \text{h.c.},\\
\mathcal{O}_{BB}^{(1)} &= \mathrm{i}H^\dagger D_\rho \widetilde{B}_{\mu\nu}B^{\mu\rho}D^\nu H + \text{h.c.}, & \mathcal{O}_{WW}^{(1)} &= iH^\dagger D_\rho \widetilde{W}_{\mu\nu}W^{\mu\rho}D^\nu H + \text{h.c.},\\
\mathcal{O}_{BB}^{(2)} &= \mathrm{i}H^\dagger D_\rho B_{\mu\nu}\widetilde{B}^{\mu\rho}D^\nu H + \text{h.c.}, & \mathcal{O}_{WW}^{(2)} &= \mathrm{i}H^\dagger D_\rho W_{\mu\nu}\widetilde{W}^{\mu\rho}D^\nu H + \text{h.c.},\\
\widetilde{\mathcal{O}}_{BW}^{(1)} &= \mathrm{i}H^\dagger D_\rho B_{\mu\nu}W^{\mu\rho}D^\nu H + \text{h.c.}, & \widetilde{\mathcal{O}}_{WB}^{(1)} &= \mathrm{i}H^\dagger D_\rho W_{\mu\nu}B^{\mu\rho}D^\nu H + \text{h.c.},\\
\widetilde{\mathcal{O}}_{BB}^{(1)} &= \mathrm{i}H^\dagger D_\rho B_{\mu\nu}B^{\mu\rho}D^\nu H + \text{h.c.}, & \widetilde{\mathcal{O}}_{WW}^{(1)} &= \mathrm{i}H^\dagger D_\rho W_{\mu\nu}W^{\mu\rho}D^\nu H + \text{h.c.}.
\end{aligned} \tag{S19}$$

We note that in addition to the above operators, there are two other operators $\mathcal{O}_{BW}^{(2)}\!=\!\mathrm{i}H^\dagger D_\rho B_{\mu\nu}\widetilde{W}^{\mu\rho}D^\nu H$ and $\mathcal{O}_{WB}^{(2)}\!=\!\mathrm{i}H^\dagger D_\rho W_{\mu\nu}\widetilde{B}^{\mu\rho}D^\nu H$ belonging to the same subclass of $H^\dagger D_\rho F_{\mu\nu}F^{\mu\rho}D^\nu H$. But, by using the Bianchi identity $D_\rho \widetilde{F}^{\mu\rho} = 0$ and integration by parts, we find that they contribute the same nTGVs as that of $\mathcal{O}_{\widetilde{B}W}$ in Eq.(2.2a). So they are not independent and thus not included in Eq.(S19). We can expand the above operators (S19) and derive their contributions to the nTGVs:

$$\begin{aligned}
\mathcal{O}_{VV}^{(n)} \;&=\; -\frac{v^2 e Z_\nu}{2s_W c_W}(a_1\partial_\rho\widetilde{A}_{\mu\nu}A^{\mu\rho} + a_2\partial_\rho\widetilde{Z}_{\mu\nu}Z^{\mu\rho} + a_3\partial_\rho A_{\mu\nu}\widetilde{A}^{\mu\rho} + a_4\partial_\rho Z_{\mu\nu}\widetilde{Z}^{\mu\rho}\\
&\quad + a_5\partial_\rho\widetilde{A}_{\mu\nu}Z^{\mu\rho} + a_6\partial_\rho\widetilde{Z}_{\mu\nu}A^{\mu\rho} + a_7\partial_\rho A_{\mu\nu}\widetilde{Z}^{\mu\rho} + a_8\partial_\rho Z_{\mu\nu}\widetilde{A}^{\mu\rho})\,,
\end{aligned} \tag{S20a}$$

$$\widetilde{\mathcal{O}}_{VV}^{(n)} \;=\; -\frac{v^2 e Z_\nu}{2s_W c_W}(b_1\partial_\rho A_{\mu\nu}A^{\mu\rho} + b_2\partial_\rho Z_{\mu\nu}Z^{\mu\rho} + b_3\partial_\rho A_{\mu\nu}Z^{\mu\rho} + b_4\partial_\rho Z_{\mu\nu}A^{\mu\rho})\,, \tag{S20b}$$

where the vertices $\mathcal{O}_{VV}^{(n)}$ are CPC and $\widetilde{\mathcal{O}}_{VV}^{(n)}$ are CPV, with the index $n = 1, 2$. In the above, the coefficients $(a_j,\, b_j)$ are given by

$$a_1 = -\frac{c_{BW}^{(1)} c_W s_W}{2} - \frac{c_{WB}^{(1)} c_W s_W}{2} + c_{BB}^{(1)} c_W^2 + \frac{c_{WW}^{(1)} s_W^2}{4}, \tag{S21a}$$

$$a_2 = \frac{c_{BW}^{(1)} c_W s_W}{2} + \frac{c_{WB}^{(1)} c_W s_W}{2} + c_{BB}^{(1)} s_W^2 + \frac{c_{WW}^{(1)} c_W^2}{4}, \tag{S21b}$$

$$a_3 = c_{BB}^{(2)} c_W^2 + \frac{c_{WW}^{(2)} s_W^2}{4}, \tag{S21c}$$

$$a_4 = c_{BB}^{(2)} s_W^2 + \frac{c_{WW}^{(2)} c_W^2}{4}, \tag{S21d}$$

$$a_5 = -\frac{c_{BW}^{(1)} c_W^2}{2} + \frac{c_{WB}^{(1)} s_W^2}{2} - c_{BB}^{(1)} c_W s_W + \frac{c_{WW}^{(1)} c_W s_W}{4}, \tag{S21e}$$

$$a_6 = \frac{c_{BW}^{(1)} c_W^2}{2} - \frac{c_{WB}^{(1)} s_W^2}{2} - c_{BB}^{(1)} c_W s_W + \frac{c_{WW}^{(1)} c_W s_W}{4}, \tag{S21f}$$

$$a_7 = -c_{BB}^{(2)} c_W s_W + \frac{c_{WW}^{(2)} c_W s_W}{4}, \tag{S21g}$$

$$a_8 = -c_{BB}^{(2)} c_W s_W + \frac{c_{WW}^{(2)} c_W s_W}{4}, \tag{S21h}$$

and

$$b_1 = -\frac{\tilde{c}_{BW}^{(1)} c_W s_W}{2} - \frac{\tilde{c}_{WB}^{(1)} c_W s_W}{2} + \tilde{c}_{BB}^{(1)} c_W^2 + \frac{\tilde{c}_{WW}^{(1)} s_W^2}{4}, \tag{S22a}$$

$$b_2 = \frac{\tilde{c}_{BW}^{(1)} c_W s_W}{2} + \frac{\tilde{c}_{WB}^{(1)} c_W s_W}{2} + \tilde{c}_{BB}^{(1)} s_W^2 + \frac{\tilde{c}_{WW}^{(1)} c_W^2}{4}, \tag{S22b}$$

$$b_3 = -\frac{\tilde{c}_{BW}^{(1)} c_W^2}{2} + \frac{\tilde{c}_{WB}^{(1)} s_W^2}{2} - \tilde{c}_{BB}^{(1)} c_W s_W + \frac{\tilde{c}_{WW}^{(1)} c_W s_W}{4}, \tag{S22c}$$

$$b_4 = \frac{\tilde{c}_{BW}^{(1)} c_W^2}{2} - \frac{\tilde{c}_{WB}^{(1)} s_W^2}{2} - \tilde{c}_{BB}^{(1)} c_W s_W + \frac{\tilde{c}_{WW}^{(1)} c_W s_W}{4}. \tag{S22d}$$

Thus, we derive their contribution to the nTGC form factors:

$$\hat{h}_3^Z = \frac{v^2 M_Z^2}{2 c_W s_W \Lambda^4} (-a_5 - a_6 - a_7 + a_8)\,, \tag{S23a}$$

$$h_{31}^{\gamma} = -\frac{v^2 M_Z^2}{c_W s_W \Lambda^4} a_1\,, \tag{S23b}$$

$$\hat{h}_1^Z = \frac{v^2 M_Z^2}{4 c_W s_W \Lambda^4} (b_4 - b_3)\,. \tag{S23c}$$

Inspecting Eq.(S20), we find that the subclass $H^\dagger D_\rho F_{\mu\nu} F^{\mu\rho} D^\nu H$ contribute the same Lorentz structures of the form factors as that of the other subclass $H^\dagger F_{\mu\nu} F^{\mu\rho} D_\rho D^\nu H$. Hence it will suffice to focus our analysis just on one kind of subclass operators $H^\dagger F_{\mu\nu} F^{\mu\rho} D_\rho D^\nu H$ in the main text.

S2. Cross Sections for CPC and CPV nTGC Contributions

In this section, we present the cross section formulae for the reaction $q\bar{q} \to Z^*\gamma$ in terms of the SM contribution (σ_0), the interference between the SM and the nTGC contributions (σ_1), and the squared part of the nTGC contributions (σ_2), which are used in Eq.(10) of the main text:

$$\sigma(q\bar{q} \to Z^*\gamma) = \sigma_0 + \sigma_1 + \sigma_2\,. \tag{S24}$$

$\sqrt{s}$	13 TeV				100 TeV		
$\mathcal{L}(\mathrm{ab}^{-1})$	0.14	0.3	3		3	10	30
$\lvert\hat{h}_{4,2}\rvert\times 10^6$	11	8.5	4.2	$\lvert\hat{h}_{4,2}\rvert\times 10^9$	4.5	2.9	2.0
$\lvert h^Z_{4,2}\rvert\times 10^6$	0.47	0.37	0.19	$\lvert h^Z_{4,2}\rvert\times 10^{11}$	2.6	1.7	1.2
$\lvert h^\gamma_{4,2}\rvert\times 10^6$	0.54	0.43	0.22	$\lvert h^\gamma_{4,2}\rvert\times 10^{11}$	2.9	1.9	1.4

Table S3: *Comparisons of the 2σ sensitivity reaches for the form factors $(\hat{h}_4, \hat{h}_2)$ formulated in the SMEFT (in red color) and for the conventional form factors (h_4^V, h_2^V) respecting only U(1)$_{\rm em}$ (in blue color), derived from the reaction $pp(q\bar{q})\to Z\gamma\to\nu\bar{\nu}\gamma$ at the* LHC (13 TeV) *and a* 100 TeV *pp collider, with the indicated integrated luminosities. As discussed in the text, the form-factor limits in blue color are included for illustration only, as they are incompatible with the spontaneous breaking of the SM electroweak gauge symmetry, and hence are invalid.*

The SM cross section term (σ_0) and the interference term (σ_1) are given by

$$\sigma_0 = \frac{e^4(q_L^2+q_R^2)Q^2\left[-(\hat{s}-M_{Z^*}^2)^2-2(\hat{s}^2+M_{Z^*}^4)\ln\sin\frac{\delta}{2}\right]}{8\pi s_W^2 c_W^2(\hat{s}-M_{Z^*}^2)\,\hat{s}^2}\,, \tag{S25a}$$

$$\begin{aligned}\sigma_1 =& -\frac{e^4 Q q_L T_3\left(\hat{s}-M_{Z^*}^2\right)}{16\pi s_W^2 c_W^2 M_{Z^*}^2\,\hat{s}}\bar{h}_4 - \frac{e^4 Q(q_L x_L^Z - q_R x_R^Z)(\hat{s}^2-M_{Z^*}^4)}{16\pi s_W^2 c_W^2 M_{Z^*}^2\,\hat{s}^2}\bar{h}_3^Z \\ &+ \frac{e^4 Q(q_L x_L^A - q_R x_R^A)(\hat{s}^2-M_{Z^*}^4)}{16\pi s_W^3 c_W M_{Z^*}^2\,\hat{s}^2}\bar{h}_3^\gamma\,,\end{aligned} \tag{S25b}$$

while the squared contribution (σ_2) includes the following terms:

$$\sigma_2 = \sigma_2^{44}+\sigma_{2Z}^{33}+\sigma_{2A}^{33}+\sigma_{2Z}^{43}+\sigma_{2A}^{43}+\sigma_{2ZA}^{33}\,, \tag{S26a}$$

$$\sigma_2^{44} = \frac{e^4 T_3^2(\hat{s}+M_{Z^*}^2)(\hat{s}-M_{Z^*}^2)^3}{768\pi s_W^2 c_W^2 M_{Z^*}^8\,\hat{s}}\left[(\bar{h}_2)^2+(\bar{h}_4)^2\right], \tag{S26b}$$

$$\sigma_{2Z}^{33} = \frac{e^4[Q^2 s_W^4+(T_3-Qs_W^2)^2](\hat{s}+M_{Z^*}^2)(\hat{s}-M_{Z^*}^2)^3}{192\pi s_W^2 c_W^2 M_{Z^*}^6\,\hat{s}^2}\left[(\bar{h}_1^Z)^2+(\bar{h}_3^Z)^2\right], \tag{S26c}$$

$$\sigma_{2A}^{33} = \frac{e^4 Q^2(\hat{s}+M_{Z^*}^2)(\hat{s}-M_{Z^*}^2)^3}{96\pi M_{Z^*}^6\,\hat{s}^2}\left[(\bar{h}_1^\gamma)^2+(\bar{h}_3^\gamma)^2\right], \tag{S26d}$$

$$\sigma_{2Z}^{43} = \frac{e^4 T_3(T_3-Qs_W^2)(\hat{s}-M_{Z^*}^2)^3}{96\pi s_W^2 c_W^2 M_{Z^*}^6\,\hat{s}}\left(\bar{h}_2\bar{h}_1^Z+\bar{h}_4\bar{h}_3^Z\right), \tag{S26e}$$

$$\sigma_{2A}^{43} = \frac{e^4 Q T_3(\hat{s}-M_{Z^*}^2)^3}{96\pi s_W c_W M_{Z^*}^6\,\hat{s}}\left(\bar{h}_2\bar{h}_1^\gamma+\bar{h}_4\bar{h}_3^\gamma\right), \tag{S26f}$$

$$\sigma_{2ZA}^{33} = \frac{e^4 Q(T_3-2Qs_W^2)(\hat{s}+M_{Z^*}^2)(\hat{s}-M_{Z^*}^2)^3}{96\pi s_W c_W M_{Z^*}^6\,\hat{s}^2}\left(\bar{h}_1^Z\bar{h}_1^\gamma+\bar{h}_3^Z\bar{h}_3^\gamma\right), \tag{S26g}$$

where the nTGC parameters

$$\bar{h}_{1,3}^Z = \hat{h}_{1,3}^Z\frac{M_{Z^*}^2}{M_Z^2}\,,\qquad \bar{h}_{1,3}^\gamma = h_{1,3}\frac{M_{Z^*}^2}{M_Z^2}+\hat{h}_{1,3}\frac{M_{Z^*}^4}{M_Z^4}\,,\qquad \bar{h}_{2,4} = \hat{h}_{2,4}\frac{M_{Z^*}^4}{M_Z^4}\,. \tag{S27}$$

In the above, the squared-mass $M_{Z^*}^2 = q_1^2$ with q_1 being the Z^* momentum, and the coefficients $(q_L,\,q_R)=(T_3-Qs_W^2,\,-Qs_W^2)$, $(x_L^Z,\,x_R^Z)=(T_3-Qs_W^2,\,-Qs_W^2)$, and $(x_L^A,\,x_R^A)=-Qs_W^2(1,1)$ denote the (left, right)-handed gauge couplings between quarks and the Z boson.

$\sqrt{s}$	13 TeV				100 TeV		
$\mathcal{L}(\text{ab}^{-1})$	0.14	0.3	3		3	10	30
$\lvert\hat{h}_{4,2}\rvert\times 10^6$	9.6	7.5	3.8	$\lvert\hat{h}_{4,2}\rvert\times 10^9$	3.9	2.6	1.8
$\lvert\hat{h}^Z_{3,1}\rvert\times 10^4$	1.9	1.5	0.80	$\lvert\hat{h}^Z_{3,1}\rvert\times 10^7$	6.1	4.2	3.0
$\lvert\hat{h}^\gamma_{3,1}\rvert\times 10^4$	1.6	1.2	0.65	$\lvert\hat{h}^\gamma_{3,1}\rvert\times 10^7$	0.94	0.62	0.44
$\lvert h^\gamma_{31,11}\rvert\times 10^4$	2.2	1.8	0.94	$\lvert h^\gamma_{31,11}\rvert\times 10^7$	7.1	4.9	3.5

Table S4: *Combined sensitivity reaches on probing the CPC and CPV nTGC form factors at the* 2σ *level, as obtained by analyzing the reactions* $pp(q\bar{q})\to Z^*\gamma\to\nu\bar{\nu}\gamma$ *and* $pp(q\bar{q})\to Z\gamma\to\ell^+\ell^-\gamma$ *at the* LHC (13 TeV) *and the* 100 TeV *pp collider, for the indicated integrated luminosities. In the last two rows, the* $\hat{h}^\gamma_{3,1}$ *sensitivities (red color) are significantly higher than those of* $h^\gamma_{31,11}$ *(blue color) because the former contains the off-shell contributions from* $\nu\bar{\nu}\gamma$ *channel as enhanced by* Z^**-momentum-square* (q_1^2) *and the latter does not.*

Finally, we combine the sensitivity reaches on probing the CPC and CPV nTGC form factors by using the bounds derived from the reaction $pp(q\bar{q})\to Z^*\gamma\to\nu\bar{\nu}\gamma$ (given in Table I of the main text) and the reaction $pp(q\bar{q})\to Z\gamma\to\ell^+\ell^-\gamma$. We analyzed the $\nu\bar{\nu}\gamma$ channel in [1] only for CPC nTGCs, and for the current combined analysis we further include the CPV nTGCs. We present the combined sensitivity reaches on probing the CPC and CPV nTGC form factors at the 2σ level, for both the on-going LHC and the projected 100 TeV *pp* collider, as shown in Table S4. We find that the sensitivity reaches on the form factors $\hat{h}_{4,2}$, $\hat{h}^Z_{3,1}$, and $h^\gamma_{31,11}$ are comparable for both $\nu\bar{\nu}\gamma$ and $\ell^+\ell^-\gamma$ channels, where the $\nu\bar{\nu}\gamma$ channel has higher sensitivities than the $\ell^+\ell^-\gamma$ channel by about $(20-30)\%$ at the LHC and the 100 TeV *pp* collider, and thus their combined sensitivities have visible improvements. On the other hand, the sensitivity reaches on the form factors $\hat{h}^\gamma_{3,1}$ via the $\nu\bar{\nu}\gamma$ channel are significantly higher than those via the $\ell^+\ell^-\gamma$ channel by about 93% at the LHC and by a large factor of ~ 11 at the 100 TeV *pp* collider, because of the major off-shell enhancement on the $\nu\bar{\nu}\gamma$ signals as we demonstrated in the main text. This explains why the combined sensitivity reaches on $\hat{h}^\gamma_{3,1}$ (shown in Table S4 and marked in red color) are dominated by the $\nu\bar{\nu}\gamma$ channel and remain nearly the same as the sensitivities of the $\nu\bar{\nu}\gamma$ channel alone (shown in Table I of the main text). We also analyzed the combined sensitivity reaches on the new physics cutoff scale Λ_j for each given nTGC operator $\mathcal{O}_j$. Since the nTGC contribution to the signal cross section is dominated by the σ_2 term which is proportional to $1/\Lambda_j^8$ (as compared to $\sigma_2\propto\hat{h}_j^2$ for the form factor contributions), we would expect a rather minor enhancement by $2^{1/16}-1\simeq 4.4\%$ even if the two channels of $\nu\bar{\nu}\gamma$ and $\ell^+\ell^-\gamma$ would contribute equal statistic significance. We present in Table S5 the combined sensitivity reaches on the new physics scales Λ_j (in TeV) of the dimension-8 nTGC operators at 2σ level. As expected, it shows that the combination of both $\nu\bar{\nu}\gamma$ and $\ell^+\ell^-\gamma$ channels leads to fairly minor improvements on the sensitivity reaches. Especially, there are essentially no visible improvements beyond the sensitivity bounds of the $\nu\bar{\nu}\gamma$ channel (shown in Table II of the main text) for new physics scales (Λ_{G-}, $\Lambda_{\widetilde{G}-}$), which correspond to the nTGC form factors ($\hat{h}^\gamma_3$, $\hat{h}^\gamma_1$). This is because the $\nu\bar{\nu}\gamma$ channel has large off-shell enhancements for the contributions of ($\hat{h}^\gamma_3$, $\hat{h}^\gamma_1$) and thus the corresponding new physics scale (Λ_{G-}, $\Lambda_{\widetilde{G}-}$), which lead to significantly higher sensitivity reaches than those of the $\ell^+\ell^-\gamma$ channel.

$\sqrt{s}$	13 TeV			100 TeV		
$\mathcal{L}\,(\text{ab}^{-1})$	0.14	0.3	3	3	10	30
Λ_{G+}(CPC)	3.4	3.6	4.2	23	26	29
Λ_{G-}(CPC)	1.2	1.3	1.5	7.7	8.5	9.3
$\Lambda_{\widetilde{B}W}$(CPC)	1.3	1.4	1.6	5.6	6.1	6.6
$\Lambda_{\widetilde{BW}}$(CPC)	1.5	1.6	1.9	6.4	7.0	7.6
$\Lambda_{\widetilde{G}+}$(CPV)	2.8	3.0	3.5	20	22	24
$\Lambda_{\widetilde{G}-}$(CPV)	1.0	1.1	1.3	6.5	7.2	7.8
Λ_{WW}(CPV)	0.96	1.0	1.2	4.0	4.4	4.8
Λ_{WB}(CPV)	1.1	1.2	1.4	4.8	5.2	5.7
Λ_{BB}(CPV)	1.4	1.5	1.7	5.8	64	7.0

Table S5: *Combined sensitivity reaches on the new physics scales* Λ_j (in TeV) *of the dimension-8 nTGC operators at* 2σ *level, as obtained by analyzing the reactions* $pp(q\bar{q})\to Z^*\gamma\to\nu\bar{\nu}\gamma$ *and* $pp(q\bar{q})\to Z\gamma\to\ell^+\ell^-\gamma$ *at the* LHC (13 TeV) *and at a* 100 TeV pp *collider, with integrated luminosities* $\mathcal{L}$ *as indicated.*

S3. Unitarity Constraints on CPC and CPV nTGCs

In this section, we analyze the perturbative unitarity bounds on both the CPC and CPV nTGCs through the on-shell scattering process $f\bar{f}\to Z\gamma$ with $f\bar{f}=q\bar{q},\, e^-e^+$. This also extends our previous unitarity analysis for the CPC nTGCs alone [1]. For the scattering amplitude of the reaction $f\bar{f}\to Z\gamma$, We make the partial-wave expansion of the nTGC contributions:

$$a_J \;=\; \frac{1}{32\pi}e^{i(\nu'-\nu)\phi}\int_{-1}^{1}\mathrm{d}(\cos\theta)\, d^J_{\nu'\nu}(\cos\theta)\, \mathcal{T}_{\text{nTGC}}^{s_f s_{\bar{f}},\lambda_Z\lambda_\gamma}, \tag{S28}$$

where the differences of initial/final state helicities are given by $\nu = s_f - s_{\bar{f}} = \pm 1$ and $\nu' = \lambda_Z - \lambda_\gamma = 0, \pm 1$, respectively. For the current collider analysis it is sufficient to treat the initial-state fermions $(f, \bar{f})$ (light quarks or leptons) as massless. So we deduce $s_f = -s_{\bar{f}}$, leading to $\nu = \pm 1$. This means that the $J=1$ partial wave gives the leading contribution. The relevant Wigner d functions are given by $d^1_{1,0} = -\frac{1}{\sqrt{2}}\sin\theta$ and $d^1_{1,\pm1} = \frac{1}{2}(1\pm\cos\theta)$, whereas the general relation $d^J_{m,m'} = d^J_{-m,-m'}$ holds.

With these, we impose the inelastic unitarity condition [22] on each given partial-wave amplitude, $|a^{\text{ine}}_J| < \frac{1}{2}$ for $J=1$, and derive the following perturbative unitarity bounds on the leading contributions of the nTGC form factors:

$$|h_{4,2}| < \frac{24\sqrt{2}\,\pi v^2 M_Z^2}{s_W c_W s^2}, \quad |h^Z_{3,1}| < \frac{6\sqrt{2}\pi v^2 M_Z}{s_W c_W (T_3 - Q s_W^2)\, s^{3/2}}, \quad |h^\gamma_{3,1}| < \frac{6\sqrt{2}\pi v^2 M_Z}{s_W^2 c_W^2 |Q|\, s^{3/2}}, \tag{S29}$$

where Q is the electric charge of the initial state fermions, $T_3 = \pm\frac{1}{2}$ for left-handed fermions, and $T_3 = 0$ for right-handed fermions. Then, we impose the inelastic unitarity condition on the

$E_{\rm CM}$ (TeV)	0.25	0.5	1	3	5	25	40
Λ_{G+}	0.078	0.16	0.31	0.93	1.6	7.8	12
Λ_{G-}	0.050	0.084	0.14	0.32	0.47	1.6	2.2
$\Lambda_{\widetilde{B}W}$	0.058	0.098	0.16	0.37	0.55	1.8	2.6
$\Lambda_{\widetilde{BW}}$	0.069	0.12	0.20	0.44	0.65	2.2	3.1
$\Lambda_{\widetilde{G}+}$	0.065	0.13	0.26	0.79	1.3	6.5	10
$\Lambda_{\widetilde{G}-}$	0.042	0.071	0.12	0.27	0.40	1.3	1.9
Λ_{WW}	0.041	0.069	0.12	0.26	0.39	1.3	1.8
Λ_{WB}	0.051	0.086	0.14	0.33	0.48	1.6	2.3
Λ_{BB}	0.069	0.12	0.20	0.44	0.65	2.2	3.1
$\lvert h_{4,2}\rvert$	33	2.0	0.13	1.6×10^{-3}	2.0×10^{-4}	3.3×10^{-7}	5.0×10^{-8}
$\lvert h_{3,1}^{Z}\rvert$	53	6.6	0.83	0.031	6.6×10^{-3}	5.3×10^{-5}	1.3×10^{-5}
$\lvert h_{3,1}^{\gamma}\rvert$	53	6.6	0.83	0.031	6.6×10^{-3}	5.3×10^{-5}	1.3×10^{-5}

Table S6: *Unitarity bounds on the new physics scale* Λ_j (in TeV) of the dimension-8 nTGC operators and on the nTGC form factors h_j^V including both the CPC and CPV cases. These bounds are derived for various sample values of the c.m. energy $E_{\rm CM}$ of the reaction $q\bar{q}\to Z\gamma$ or $e^-e^+\to Z\gamma$ that are relevant to the present collider study.

contribution of each dimension-8 nTGC operator to the partial wave amplitude of the reaction $f\bar{f}\to Z\gamma$, and derive the following perturbative inelastic unitarity bounds:

$$\Lambda_{G+} > \frac{\sqrt{s}}{(24\sqrt{2}\,\pi)^{1/4}}\,, \qquad \Lambda_{G-} > \left(\frac{s_W^2|Q|M_Z}{12\sqrt{2}\,\pi}\right)^{\frac{1}{4}}(\sqrt{s}\,)^{\frac{3}{4}}, \quad \Lambda_{\widetilde{B}W} > \left(\frac{|\widehat{T}_3|M_Z}{12\sqrt{2}\,\pi}\right)^{\frac{1}{4}}(\sqrt{s}\,)^{\frac{3}{4}}, \tag{S30a}$$

$$\Lambda_{\widetilde{BW}} > \left(\frac{2|Q|M_Z}{\omega}\right)^{\frac{1}{4}}(\sqrt{s}\,)^{\frac{3}{4}}, \quad \Lambda_{\widetilde{G}+} > \frac{\sqrt{s}}{(48\sqrt{2}\,\pi)^{1/4}}\,, \qquad \Lambda_{\widetilde{G}-} > \left(\frac{s_W|Q|M_Z}{2c_W\,\omega}\right)^{\frac{1}{4}}(\sqrt{s}\,)^{\frac{3}{4}}, \tag{S30b}$$

$$\Lambda_{WW} > \left(\frac{|T_3|M_Z}{2\omega}\right)^{\frac{1}{4}}(\sqrt{s}\,)^{\frac{3}{4}}, \quad \Lambda_{BW} > \left(\frac{|\widehat{Q}|M_Z}{2s_Wc_W\omega}\right)^{\frac{1}{4}}(\sqrt{s}\,)^{\frac{3}{4}}, \quad \Lambda_{BB} > \left(\frac{2|Q-T_3|M_Z}{\omega}\right)^{\frac{1}{4}}(\sqrt{s}\,)^{\frac{3}{4}}\,, \tag{S30c}$$

where we have defined $\omega = 12\sqrt{2}\pi/(s_Wc_W)$, $\widehat{T}_3 = T_3 - Qs_W^2$, and $\widehat{Q} = Qs_W^2 + T_3(1-2s_W^2)$. With these we derive the numerical unitarity bounds on the new physics scale Λ_j of each nTGC dimension-8 operator and on each nTGC form factor h_j^V, including both the CPC and CPV cases. We summarize these unitarity bounds in Table S6 for a set of sample values of the relevant center-of-mass energy $E_{\rm CM}(=\sqrt{s}\,)$ of the scattering process $f\bar{f}\to Z\gamma$ with $f\bar{f} = q\bar{q},\, e^-e^+$. Table S6 demonstrates that these unitarity bounds on Λ_j and h_j^V are much weaker than our current collider bounds (shown in Tables I-II of the main text and in Tables S4-S5 of this section) and thus do not affect our collider analyses.